HOLSEA-NL: Holocene water level and sea-level indicator dataset for the Netherlands

Kim de Wit[1], Kim M. Cohen[1], Roderik S. W. van de Wal[1,2]

[1]Department of Physical Geography, Utrecht University, P.O. Box 80.115, 3508TC Utrecht, the Netherlands
5 [2]Institute for Marine and Atmospheric research Utrecht, Utrecht University, 3584 CC Utrecht, the Netherlands

Correspondence to: Kim de Wit (k.dewit@uu.nl)

Abstract. Deltas and coastal plains worldwide developed under the influence of relative sea level rise (RSLR) during the Holocene. In the Netherlands, Holocene RSLR results from both regional sea-level rise and regional subsidence patterns, mainly caused by glacial isostatic adjustment (GIA: Scandinavian forebulge collapse) and longer-term North Sea Basin
10 tectono-sedimentary subsidence. Past coastal and inland water levels are preserved in geological indicators marking the gradual drowning of an area, for example basal peats. Such geological water-level indicators have been used in the Netherlands for varying types of research. However, uniform overviews of these data exist only for smaller local subsets and not for the entire Netherlands. In this paper we present a data set of 712 Holocene water-level indicators from the Dutch coastal plain that are relevant for studying RSLR and regional subsidence, compiled in HOLSEA workbook format (De Wit and Cohen, 2024). This
15 format was expanded to allow for registering basal-peat type geological indicators, documenting Dutch-setting specific parameters and accompanying uncertainties, to assess indicative meaning, and to appropriately correct the raw vertical positions of the indicators. Overall, our new, internally consistent, expanded documentation provided for the water-level indicators encourages users to choose the information relevant for their research and report RSLR uncertainties transparently. From the indicators, 59% was collected in 1950-2000, mainly in academic studies and survey mapping campaigns; 37% was
20 collected in 2000-2020 in academic studies and archaeological surveying projects, 4% was newly collected (this study), the latter mainly in previously under sampled central and northern Netherlands regions. Prominent regional differences exist in the vertical position and abundance of the indicators. Older indicators in our data set are mostly located in the deeper seaward area of the Netherlands. These indicators correspond well with previous transgression reconstructions, that are partly based on the same data. The younger, landwards set of indicators in the Rhine-Meuse central and Flevoland regions corresponds with
25 the transgression phase reaching further inland, from 8000 cal. BP onwards. Northern indicators of Middle Holocene age (8-5 ka cal. BP), in general lie 2-3 meters lower compared to those in the south. For younger data this difference is less, showing spatial and temporal variation in RSLR throughout the Netherlands.

1 Introduction

Holocene water-level indicators have been the subject of research in the Netherlands for decades. Previous studies collected
30 geological water-level indicators for relative sea-level reconstructions (Jelgersma, 1961; Van de Plassche, 1982; Hijma and
Cohen, 2019), geological mapping of the Dutch coastal-deltaic plain (e.g. Berendsen and Stouthamer, 2002), wetland
palaeoenvironmental reconstructions (e.g. Vos, 2015), and archaeological excavation and dating (e.g. Verbruggen, 1992).
These activities resulted in the accumulation of an extensive amount of primary water level indicator data (e.g. Jelgersma,
1961; Van de Plassche, 1982; Meijles et al., 2018; Hijma and Cohen, 2019; Quik et al., 2022). Geological water-level indicators
35 also carry information for studying various types of subsidence, namely their depth positions with increasing age as well as
the local and regional variabilities therein (Kiden et al., 2002; Cohen, 2005; Van Asselen, 2011; Koster et al., 2017). The total
reconstructed relative water-level rise signal can be separated into a Holocene water level rise and a land subsidence history.
This is possible by evaluating geological records in combination with independent sea-level and subsidence reconstructions,
and geophysical modelling simulation output. As such, subsets of water-level indicators are used to verify location-specific
40 RSLR output of glacio-isostatic adjustment (GIA) modelling, which incorporate ice sheet deglaciation history and Earth-
rheology models to resolve RSLR globally (Lambeck, 1995; Kiden et al., 2002; Shennan and Horton, 2002; Vink et al., 2007;
Bradley et al., 2011).

The abundance of geological palaeo-water level observations in the Netherlands creates a unique opportunity to study
45 Holocene differential subsidence across the entire coastal plain. Currently, an integrated overview of the geological indicator
data with consistent documentation is lacking, mainly due to the above-mentioned diversity in data usage purposes. To bridge
this gap, we created a systematic overview of the current vertical position of geological indicators; applied a uniform set of
consecutive vertical corrections, such as for water depth and compaction; and constructed a consistent error propagation
workflow. The aim of this paper is to present this newly compiled dataset of water-level indicator points, serving the study of
50 regional relative sea-, and groundwater-level rise in the Netherlands over the Holocene, and generically disclosing and
arranging this rich data for inclusion in European and global scale Holocene RSLR and coastal plain accommodation studies.

Building on previous work, the geological data compilation included a focused review of the usability of legacy data for
relative water-level reconstructions. The documentation follows the HOLSEA workbook format for Holocene relative sea-
55 level data (Hijma et al., 2015; Khan et al., 2019). The HOLSEA workbook is a versatile data reporting format that includes
correction specifications and metadata (e.g. Hijma and Cohen, 2019; Bungenstock et al., 2021; Creel et al., 2022). It categorizes
relative sea-level data entries in 'sea-level index points' (SLIPs), sea-level position bounding 'upper limiting data' (ULD) and
'lower limiting data' (LLD).

60   From our study area, a subset of 104 basal peat dates from the Rhine's lower delta was previously compiled and published in HOLSEA format (Hijma and Cohen, 2019): their 'Rotterdam' data set). Hundreds of similar dates containing potential SLIP, ULD and LLD information, which were not yet compiled, assessed, and disclosed in HOLSEA format, exist in publications from the 1950s-2010s, institutional databases, contextual reports and as unpublished data. To fill this gap, this paper expands the HOLSEA format covered data from the Netherlands to a total of 712 samples, further referred to as the HOLSEA-NL data

65   set.

While compiling the HOLSEA-NL data set, attention was given to enhancing data usability. First, various vertical correction components are specified that a user can choose to apply, such as fen/swamp water depths, peat decompaction, palaeo-tidal range and long-term background land motion. Next, the indicative meaning of the water-level indicators was reviewed to

70   assess which samples are SLIPs, ULD and LLD. Of these, the ULD category was expanded to allow for characterizing various groundwater level data points, which are relevant for reconstructing delta plains and inner lagoon peat land fringe regions as well as identifying regional trends of subsidence (e.g. Cohen, 2005). The indicative meaning of water-level indicators differs per type of deposit and past geographical setting. It is determined based on the sedimentary and biotic facies, the succession criteria on individual geological sampling locations, the spatial position of the sample and criteria on ensembles of samples

75   (e.g., outlier analysis, seaward locations priority over inland locations). Lastly, using the indicative meaning, the indicator sample depth can be updated to a past ground water level (GWL). For SLIPs and tidally linked ULD and LLD, the past GWL can be upgraded to a past mean sea level (MSL), which is referred to as a relative sea level (RSL), relative to present-day MSL. To account for the different reference water levels (RWL), we documented both the GWL and the RSL in our data set.

80   The paper proceeds further as follows: Section 2 provides an overview of the study area and its geological setting. In section 3 to 6 the set-up of the data set is described. Section 3 describes the data inventory, including data requirements and a description of different indicator types. Details on the age-depth positions, the systematic vertical corrections and additional optional adjustments are covered in Sect. 4. Section 5 presents an overview of the data, with regional and categorical breakdowns. The last section discusses potential applications and limitations of the data.

85   **2. Study area and geological setting**

The Netherlands is located in the southern part of the North Sea Basin. During the Holocene this area was strongly influenced by the RSLR resulting from the deglaciation of land ice, and regional subsidence caused by the sinking of the North Sea sedimentary Basin (Kooi et al., 1998) and glacial isostatic adjustment (GIA) remaining from the last glacial period (Lambeck, 1995; Kiden et al., 2002; Vink et al., 2007; Bradley et al., 2011). The relatively shallow depth of the southern North Sea and

90   the variation in sediment fluxes throughout the Holocene played an important role in the development of the coastal area of the Netherlands. This setting and sedimentation history also determined how and when different water level indicators could

form and therefore is relevant context for understanding the variability in indicative meaning of geological water-level indicators (Sect. 3-5). Whenever a peat layer formed on top of consolidated sediments in favourable landscape conditions (see Sect. 3), and was preserved and sampled (Sect. 1), it is suitable as a water level rise indicator (SLIP, ULD primary (= tidal),

95   ULD fluvial, ULD local inland in Fig. 2), and in some cases even as sea-level indicator (LLD, SLIP, ULD primary in Fig. 2). The geological development of the Netherlands is based on hundreds of thousands borehole observations, thousands of radiocarbon dates, further dating, and paleoenvironmental evidence, collected in parallel regional and national campaigns by multiple surveying agencies (Pons and Wiggers, 1960; Zagwijn, 1986; Berendsen and Stouthamer, 2001; Van der Meulen et al., 2013; Vos, 2015; Cohen et al., 2017a, b; Pierik and Cohen, 2020). An important aspect of these studies was to provide

100   insight in the timing and the rates of water level rise by dating coastal peats (basal and intercalated; transgressive and regressive). As a result, a detailed reconstruction of peat formation and further Holocene development in the Dutch coastal plain is possible.

At the onset of the Holocene (11,650 cal. BP), the water level in the North Sea was still low with the shallow southern sea

105   floor largely exposed. Pleistocene deposits constituted the Netherlands in the form of periglacial aeolian dune fields, cover sands, and river valleys dissecting older terraced plateaus and hills (Figure 1a; Figure 2a). Below the Holocene coastal plain of the western Netherlands, two East-West running Late Pleistocene valleys (palaeovalleys) are of relevance (Busschers et al., 2007; Vos, 2015; Peeters et al., 2016; Koster et al., 2017)). As they are the lowest elevated areas, they were first to be affected by marine transgression and hence they developed the thickest Holocene records: The southern one hosted the Rhine-Meuse

110   system of the time, which was joined by Scheldt in the near offshore. The northern one was drained by the Overijsselse Vecht underfit system (Figure 1a). Locally, inland dunes formed along river channels of each of these systems (Bennema and Pons, 1952; Wiggers, 1955; Gotjé, 1993; Berendsen and Stouthamer, 2001; Wolfert and Maas, 2007; Kasse and Aalbersberg, 2019), features that Holocene water-level rise studies have specifically targeted (see below). Below the northern coastal plain, smaller palaeo-valley systems of the Boorne and Hunze and Ems system are featured (e.g. Vos, 2015; Meijles et al., 2018). Interfluve

115   relief in the north shows push-complexes and a main till-sheet that are remnant of glaciation and deglaciation in the Saalian (the penultimate ice age; ca. 150,000 year ago, within MIS6). The latter till sheet, called the 'Drenthe plateau' (Figure 1a), forms a shallow aquitard, affecting pre-transgression groundwater tables (Van den Berg and Beets, 1987; Quik et al., 2021). Present day relief expression of the till sheet in the North, the central ice-pushed ridge complex and southwest Pleistocene fluvial terraces, determined the inland boundary of the area of interest in this paper (Figure 1b).

120
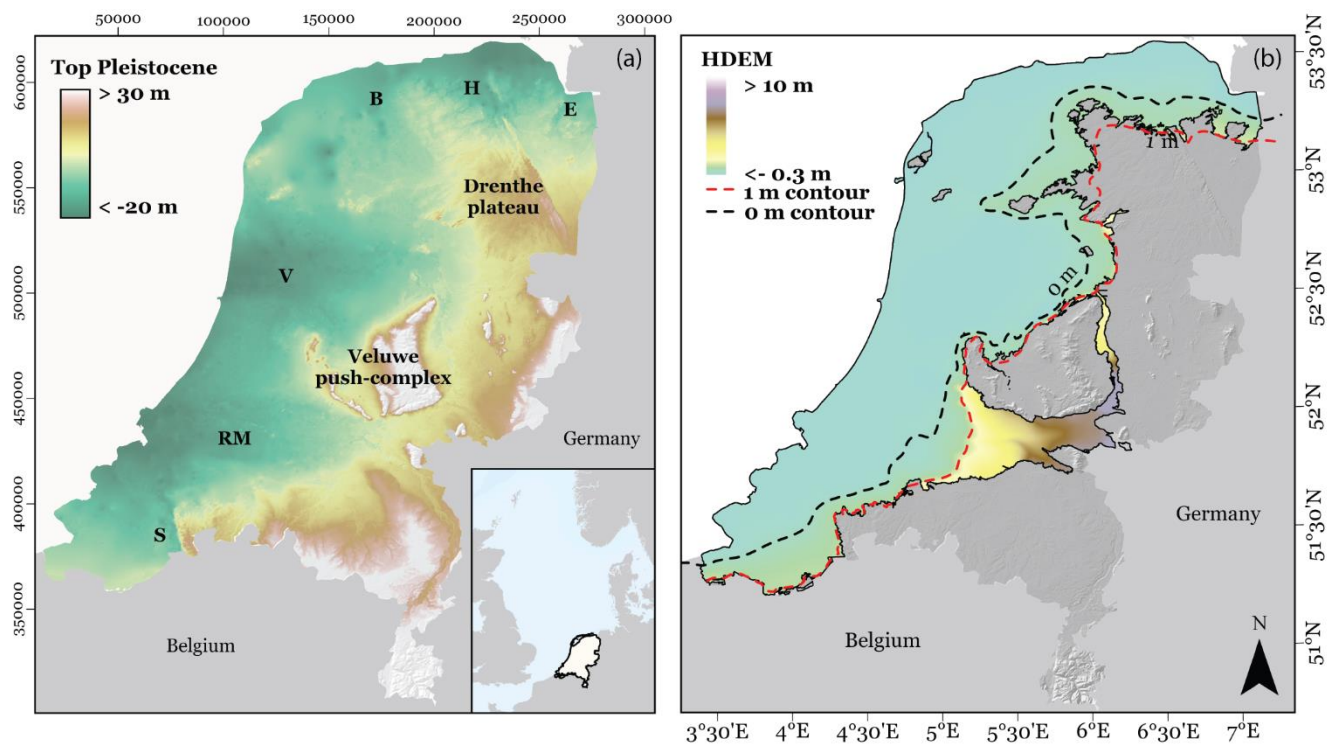
Figure 1 (a) Digital elevation model of the top of Pleistocene deposits, corrected for Holocene erosion (Cohen et al., 2017b, a; Koster et al., 2017). The labels show the location of several palaeo-valleys, B: Boorne, H: Hunze, E: Ems, V: Vecht, RM: Rhine-Meuse, S: Scheldt; (b) High stand digital elevation model (HDEM), regional groundwater table surface reconstructed for 1000 cal. yr. BP (Cohen, 2005; Cohen et al., 2017a, b; locally modified). The 0 m MSL contour (black dashed) and +1 m MSL contour (red dashed) are shown. The study area contour is adopted from Pleistocene landform outlining in national geomorphological and archaeological landscape mapping (as in Cohen et al., 2017a, b) and outside the Rhine-Meuse delta roughly coincides with the +1 m elevation contour line. Projection: RD (EPSG 28992)

125
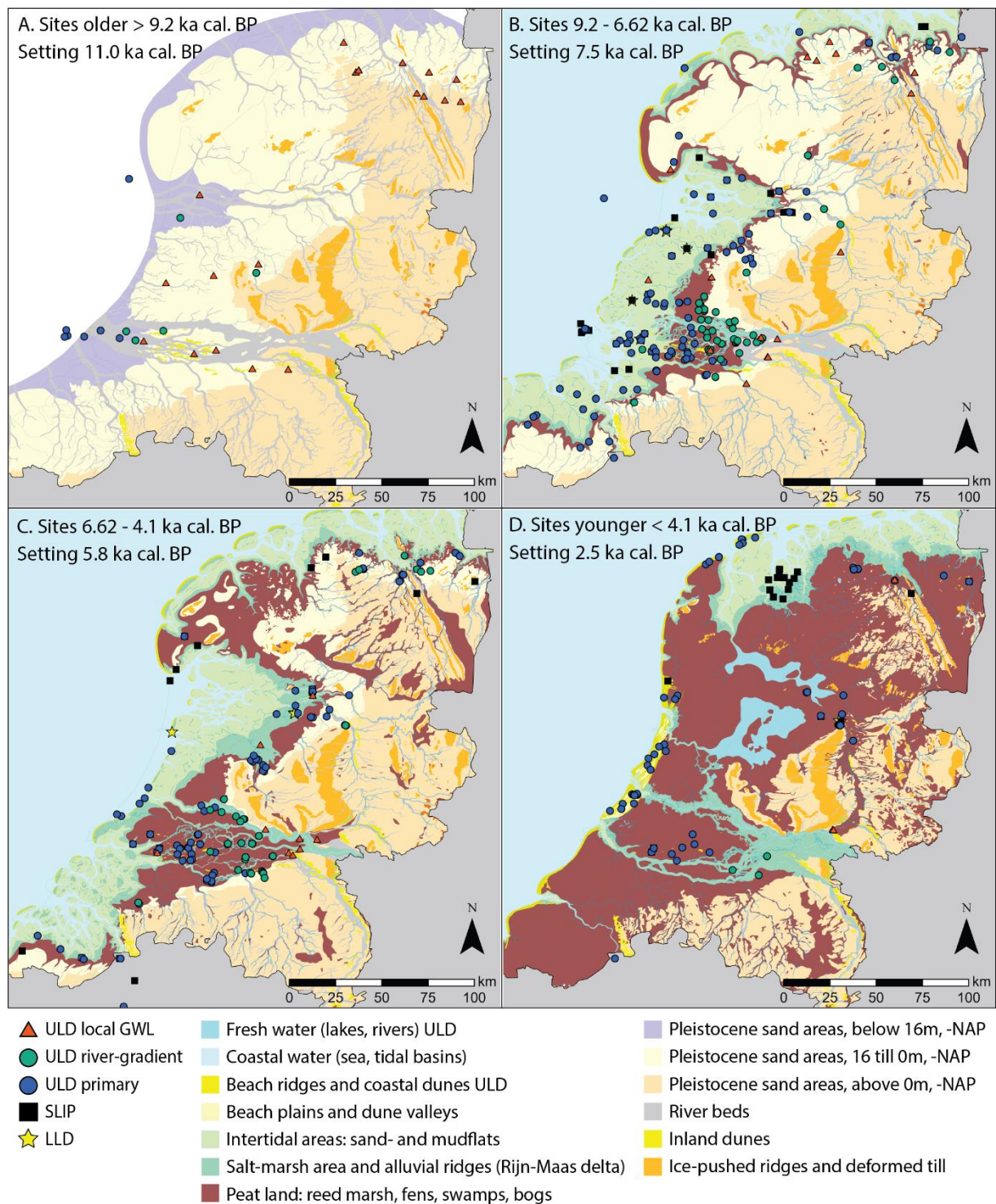
Figure 2 Geological water-level indicator site locations (this paper and data set) plotted over a national palaeogeographical map series (Vos et al., 2020), split for four time slices. The indicators shown have an age surrounding the date stamp of each selected map.

During the Early Holocene (11.6 – 8.3 ka cal. BP), the sea level increased from 60-50 m to approximately 25-20 m below the current MSL, which steadily inundated the Southern North Sea, eventually establishing coastlines in the vicinity of the modern one. River waters and inland flood basin groundwater tables were affected by the downstream rise, resulting in a decrease of the river gradient and concurrent rise of the inland groundwater levels. This initiated the growth of peat in swamps and fens

135   on former floodplains and along the drowning valley edges. From dating such transgressive peats ('basal peats'), overlain by later marine deposition, earliest water-level indicators are obtained in the near offshore (Figure 2a), and eventually across the study area, following the palaeo-valleys as gateways for the transgressive peats (Figure 2b).

As the Middle Holocene (8.3 – 4.2 ka cal. BP) commenced, the decelerating sea-level rise pushed the transgression further

140   landwards, as is evident from basal peats buried by tidal muds. Simultaneously, a beach barrier system and back-barrier Rhine-Meuse delta established (Figure 2b,c) (Berendsen and Stouthamer, 2002; Vos, 2015). The former valleys became tidal-dominated embayments, with intertidal shoals and fringing supratidal marshlands on the landward side (Figure 2b,c). This changed when the beach ridge complex matured during the Middle Holocene. The decreasing rate of sea-level rise and the supply of sediments caused most inlets of the Western Netherlands coastline to close around 5.8 ka cal. BP (Figure 2c) (Beets

145   and Spek, 2000; Hijma & Cohen, 2011). These developments and the water supply from the Rhine-Meuse delta helped turning the back-barrier area into a freshening lagoon in which widespread peat formation initiated. Areas just north remained tidally dominated for some 1500 years longer. The flood basin of the so-called Bergen tidal inlet transformed into a lagoon, gradually developing an expanding freshwater peat rim (Figure 2c) as the inlet decreased in size from 5 ka cal. BP onwards (Beets and Van der Spek, 2000). Around 3.5 ka cal. BP, also the tidal inlet of Bergen finally closed, promoting further spread of peat land

150   in the coastal plain (Figure 2d). In the very north, a series of tidal inlets remained functional, because of the relatively stronger subsidence and relative lack of sediment supply to this area. These features still persist today and are observed as the several inlets separating the Frisian Islands. The adjacent tidal basins form the Wadden Sea, its supratidal salt marshes and coastal peatlands currently bordering the mainland of the Northern Netherlands (Figure 2d). Although peat formation continued, it is difficult to find young peat layers (< 2.5 ka ca. BP). This is because many of the young peat layers disappeared, partly due to

155   erosion by rivers or the sea, but predominantly due to large-scale peat excavations that occurred since the Middle Ages when peat was mined extensively (Pierik et al., 2017). Human activity also caused large scale soft soil subsidence. This is still ongoing, mainly caused by the lowering of the groundwater level, resulting in compaction of clay and peat and peat oxidation (Van Asselen, 2011; Erkens et al., 2016). To minimize the influence of soft soil subsidence on the elevation of the water level indicators, mainly basal samples were selected.

160

In summary, during the Holocene peat formed in abundance throughout most of our study area. From 9.2 till 5 ka cal. BP under transgressive influences, lasting longest in the North and from 5.5 ka cal. BP onwards under regressive circumstances, starting from the south and moving northwards. Much of the peat from the younger period disappeared, mainly due to human activity in the past 1000 years, leaving a gap in the record for the most recent period.

3. Data inventory and intake

The water-level indicators collected in the Netherlands for different purposes over the past decades (Sect. 1), are of different types, but in great majority (640 out of 712 entries in the database) consist of sampled and dated basal peat layers from a range of settings (Figure 3). In coastal areas the dated contact of basal peat layers burying older substrate, has long been used as indicator in sea-level research, notably where basal peat could be collected along flanks of inland dunes (Sect. 2) (e.g. Jelgersma, 1961; Van de Plassche, 1982; Hijma and Cohen, 2019). Just as well, dating of the contact of the basal peat top with transgressive muds has been used as such (Hijma and Cohen, 2010, 2019). In archaeological studies, the ages of basal peat layers help to constrain the ages of archaeological findings, again notably on inland dunes (Verbruggen, 1992). In addition, basal and intercalated peat layers have been collected to determine the timing of branch avulsions in the Rhine delta and compare channel sedimentation levels with contemporary flood basin water levels (Stouthamer and Berendsen, 2000; Berendsen and Stouthamer, 2001). Intercomparison of dates from basal and intercalated positions have been used for studying auto-compaction in unconsolidated sediments (Van de Plassche, 1980; Van Asselen et al., 2009; Van Asselen, 2011). This section describes the requirements applied for selecting the legacy data, to ensure a uniform input relevant for relative water-level reconstruction research. The second part of this section gives a description of the main types of water level indicators included in the data set.

3.1 Data requirements

Basal peat beds and contacts have been the preferred geological water-level indicators, because of the combination of their radiocarbon dating potential (see below) and the fact that the projected vertical position of the indicator is minimally influenced by post-depositional compaction processes, especially those resting on a palaeosurface in sandy Pleistocene substrate. Provided that the basal peat bed is up to a few decimeters thick, this applies to indicator levels sampled from the base, middle and top of the peat bed (e.g. Hijma and Cohen, 2019). Vertical decompaction-correction and the associated uncertainty is smallest for base basal peat dates (decompaction uncertainty ~10 cm; Berendsen et al., 2007). Given the wealth of basal peat data available (research cited in Sect. 1), samples from intercalated peat layers from shallower positions than the basal peats have been excluded here because of the larger decompaction uncertainty associated with these samples. In some areas, relatively inland, peaty beds overlying the Pleistocene subsurface can reach a considerable thickness. From such peats, only levels sampled within 1 m from the Pleistocene substrate were included.

The inland boundary of the study area (Figure 1b) further constrains whether data are included. Studies sampling peat at inland locations above +1 m MSL have generally been excluded from the inventory, as peat formation there is often linked to locally perched groundwater levels and fluctuations therein (e.g. Hoek, 1997; Quik et al., 2021), in particular for areas in the north of the Netherlands with glacial till in the subsurface. Similarly, samples from pingos were excluded as well. In contrast, the coastal plain water levels are graded to the regionally increasing water level resulting in suitable regional water level indicators

(Van de Plassche, 1995). In the Rhine-Meuse river valley samples up to the 10 m contour line have been included. Previous studies have shown that these type of samples show a regional trend in groundwater level as well, which can be linked to the sea-level and subsidence history and the evolution of the area from flood basins, to tidal inlets, closed lagoons and large scale
200   peatlands (Van Dijk et al., 1991; Cohen, 2005).

The study area is further bounded towards the offshore (e.g. Figure 2a,b), where the inventory cut off has been arbitrary. The dataset contains some basal peat sampled off the Holland coast and in the Wadden Sea – as did recent regional compilation studies for these sectors (resp. Meijles et al., 2018; Hijma and Cohen, 2019). Besides, the study area is bounded by national
205   borders at critical locations in the southwest (Flanders, Belgium) and in the northeast (Niedersachsen, Germany). Where Holocene fill of palaeovalleys extended across borders, legacy data was included to allow cross-verification with data from within the study area. This is the case for a few data points from the Scheldt (following Kiden et al., 2002) and Ems palaeovalleys (following Behre, 2007).

210   A last physical boundary is the upper limit where basal peat layers can be found, which is not a prescribed boundary but a consequence of the reclamation history of the study area (see Sect. 2): extensive peat excavation since 1000 years ago has degraded Late Holocene peats top down, which imposes a soft (i.e. spatially variable) upper temporal boundary making basal peat samples younger than 3500 years rare and younger than 2500 years very rare (Van de Plassche, 1982; Cohen, 2005). To overcome this limitation, some non-basal peat sea-level index-points (13 dated shells sampled from below soles of raised
215   mounts; Frisian terp archaeological sites) were included in the data set (Vos and Nieuwhof, 2021).

To conclude, the availability of metadata played an important role in including data in the data base. An effort was made to trace the missing information, and when successful the datapoints were added. Retracing age-depth data and meta-information included information on originally applied vertical offsets and corrections, to compare this with the uniformly applicated and
220   recalculated corrections in the HOLSEA workbook. Further information was retraced to specify and calculate the uncertainty of different components. Points with insufficient information on location, depth and age determination, and associated uncertainties were left out.

3.2 Reported sampling methods and depth accuracy

225   The primary depth information in the dataset includes measurements of the surface elevation, the sample depth along the core and the thickness of the subsampled layer. This is stored in standard fields of the HOLSEA workbook, together with uncertainties and meta-information on the type of coring and type of surface elevation measurement (e.g., levelled to a benchmark, national LiDAR-datasets derived). The vertical datum to which depth is expressed is the Dutch national datum (NAP), which is approximately equal to 20th cy MSL (e.g. Vermeersen et al., 2018).

230 Basal peats have been sampled using a variety of methods, such as hand coring, mechanical coring or excavation. The sampling method and elevation determination method affect the specification of the sample depth below surface elevation and different uncertainties are associated with different methods. The uncertainties related to determining the absolute elevation of a core or section were assigned based on acquisition method, when not previously reported (e.g., levelling: ±0.02; and since the 21st century DGPS: ±0.01). The HOLSEA workbook provides a detailed breakdown of uncertainties related to sample acquisition.

235 Often sampling (e.g., levelling and benchmark) uncertainty is combined in a single value, resulting in seemingly different uncertainty values. However, added up the total vertical uncertainties related to sample acquisition add up to similar values as previously reported.

For determining the depth of a sample in a core or section, the uncertainties are assigned separately. The overall error related

240 to measuring the sample depth in the core (sample-position accuracy) was set at 0.02 m following the estimated error found by Berendsen et al. (2007) when sampling from a core. For hand-cored samples non-vertical drilling offsets are accounted for by adding an additional unidirectional uncertainty of -0.02 m per meter coring depth (Törnqvist et al., 2004; Hijma and Cohen, 2019), increasing only the upward component of the total vertical error. Depth uncertainty due to core shortening/stretching during sampling and initial storage is separately considered. This is set to ±0.05 m for hand and mechanically collected cores

245 alike, following Hijma and Cohen (2019).

In general, the depth uncertainty terms combined are smaller than the offsets and uncertainties depending on assigned indicative meaning (Sect. 3.3 and Sect. 4.2), decompaction (Sect. 4.1) and further vertical position corrections (Sect. 4.3 and 4.4). The exception are the samples taken offshore, for which the depth uncertainty terms are higher due to the additional water

250 depth uncertainty. For basal peat samples ultimately classified as SLIPs, the depth uncertainty terms account for about 20% of the total uncertainty, while for basal peat samples ultimately classified as ULD this accounts for about 25%.

3.3 Indicative meanings

Indicative meaning refers to the relation between the depth of deposition of the indicator and the water level at the time of deposition (Shennan, 1982; Van de Plassche, 1986; Hijma et al., 2015). Where it regards the indicative meaning of sampled

255 basal peat, the type of peat collected (botanical composition, sedimentology, clastic admixture) as well as aspects of geological setting (location in palaeolandscape and associated hydrological regime) contribute to specifying the indicative meaning of that sample. Bos et al. (2012) provided a classification key for organics and an overview of the distribution of basal peats underlying the Rhine-Meuse delta. They mapped the different facies (peat types) and distinguished between tidally (reed, clayey), river-flooding (woody), and seepage- or precipitation-dominated (fens, bogs) hydrological regimes in the downstream,

260 inland, and rim sectors of the Rhine-Meuse palaeovalley, respectively. Van de Plassche (1982, 1986), Kiden (1995), Kiden et al. (2002), Makaske et al. (2003) and Van de Plassche et al. (2005, 2010) developed generic indicative meaning attribution schemes for Dutch settings, which were further developed for the Rhine-Meuse basal peats by Cohen (2005), Berendsen et al.

(2007) and Hijma and Cohen (2019). In HOLSEA terms: any basal peat sample can be attributed a GWL related indicative meaning forming an upper limit to MSL, an ULD. In specific cases these can be upgraded to a sea level related indicative
265   meaning, allowing to define a SLIP.

3.3.1 GWL vs. MSL indicative meaning

The diverse peat types that make up basal peat beds formed under different hydrological regimes with varying year-round water depths (e.g., woody swamps, reed marshes, sedge fens, mossy blanket bogs). For this reason, each sample is assigned an indicative meaning and indicative range according to Table 1 (Törnqvist et al., 1998; Makaske et al., 2003; Cohen, 2005;
270   Berendsen et al., 2007; Bos et al., 2012; Hijma and Cohen, 2019). Based on that indicative meaning, the reference water level (RWL) is calculated, which represents the height of the water level at the time the water-level indicator was formed. The RWL is the midpoint of the indicative range (IR). This classification is the first step for relating the sample to a former GWL level. The second step is to determine if the GWL can also be related to a marine RWL such as Mean High Water (MHW). If this is the case, the sample is related to a past MSL based on palaeo-tidal conditions (Sect. 4.1.2), and a SLIP is defined. The indicative
275   water depth specifications of each peat type thus propagate into the eventual age-depth values as one of several vertical corrections terms. Table 1 also includes organic subaquatic gyttja deposits, which are LLD and potential SLIP data points, when encountered topping basal peats (3 out of 32 gyttja samples in the dataset). For brackish mollusca and charcoal beds traced along dune flank the indicative meaning is determine separately per case, thus those are excluded from this table.

280   Table 1 lists standard values for water depth and associated uncertainty per peat type, as well as how this is relates to ULD, SLIP or LLD classification. The latter classification is determined by evaluating peat bed thickness, sample position (Sect. 3.3.1), bed lithology, botanical composition (Table 1), and further considerations of stratigraphic and geographic position of the sample (setting) – usually with some iterative cross-checks (Hijma and Cohen, 2019). First, all basal peat samples are regarded as groundwater index points (RWL = GWL). Second, the group is divided into a seaward and shallower/younger
285   subset, and an inland and deeper/older subset, based on geographic location and age-depth information as a starting assumption, further improved by iterative comparison with surrounding age-depth data. For the seaward, younger/shallower subset, the GWL can be regarded as controlled by tidal waters, and therefore relatable to sea-level (RWL = GWL = MHW; Van de Plassche, 1995; Shennan et al., 2000). For the inland, deeper/older subset, GWL is considered otherwise controlled and to have been positioned well above contemporary MHW levels (Van Dijk et al., 1991; Van de Plassche, 1995; Cohen, 2005; Vis et al.,
290   2015; Hijma and Cohen, 2019).

Table 1 Indicative meanings for various peat and organic facies, for ULD, SLIP and LLD entries (after Hijma and Cohen, 2019).

Sedimentary indicator facies 'peat type' (Field 54)	# entries (N=670)	Palaeo-water-depth	Sample indicative meaning (Field 56)			IR uncertainty (Field 58)
			ULD vertical positioning	SLIP vertical positioning	LLD vertical positioning	Palaeo-water-depth uncertainty
Bog peat	5	0	GWL			± 0.1
Fen-wood peat	252	0	GWL	MHW		± 0.1
Fen peat on inland dune flanks	56	0	GWL-0.1	MHW-0.1		± 0.2
Fen-bog peat	2	0.3	GWL-0.3	MHW-0.3		± 0.2
Fen peat	167	0.3	GWL-0.3	MHW-0.3		± 0.2
Undifferentiated peat types	145	0.2	GWL-0.2	MHW-0.2		± 0.3
Gyttjaic organic beds	24	0.75	GWL-0.75	MHW-0.75		± 0.5
Organic detritus/clay	8	0.75	GWL-0.75	MHW-0.75	MSL-0.75	± 0.5
Other (includes: palaeosols, other drowned surfaces)	11	other				other

3.3.2 Base basal peat, Top basal peat

295   As introduced in Sect. 2, SLR during the Middle Holocene caused a concurrent rise of the coastal groundwater levels up to tens of kilometres landward (Jelgersma, 1961; Van de Plassche, 1982; Van Dijk et al., 1991; Cohen, 2005; Koster et al., 2017). This drove zonal paludification (i.e., extensive peat growth) of the Pleistocene subsurface underlying the eventual Dutch coastal plain. The so-called basal peats that formed this way are of variable botanical composition (Bennema, 1954; Van de Plassche, 1982; Cohen, 2005; Bos et al., 2012). The very base of the peat bed overlying the Pleistocene substrate (Figure 3b)

300   is regarded to mark the beginning of peat formation: the organic facies reflect that year-round swampy to marshy conditions have established at that location, and radiocarbon dating of these facies reflects when this occurred. Together, the age-depth data thus pin a past GWL position, that in river mouth and lagoon rim situations in turn provides an upper limit to the sea level position of that time (Berendsen et al., 2007; Hijma and Cohen, 2010, 2019; Van de Plassche et al., 2010; Koster et al., 2017; Meijles et al., 2018; Quik et al., 2022). This base-basal peat sample context and index-point use concept applies to 622 of the

305   640 basal peat datapoints (incl. 105 SLIPs, 337 tidal ULD), dated at the base or in the middle of the peat bed.

   A variant is to date samples from the very top of a basal peat bed where it is overlain by tidal clays (Figure 3b), preferably in addition to dating the base of the peat bed. This then provides a second age-depth water level index point, more directly marking the marine inundation of a young peatland surface just above the older subsurface. This sampling context and index-point concept applies to ~50 of the 640 basal peat datapoints. Decompaction offsets and uncertainties (see Sect. 4) are larger

310   for these top basal peat points, which propagates in the vertical accuracy of the water level index point (e.g. Makaske et al.,

2003; Berendsen et al., 2007; Hijma and Cohen, 2019). The indicative meaning based on peat composition (Table 1) is assigned indifferently of base, mid and top sampling.

3.3.3 Data points from peat beds on inland dune flanks

Section 2 introduced inland dunes as part of the Rhine-Meuse and Overijsselse Vecht palaeo-valley substrate (Fig. 1a). These dunes formed in the Late-Glacial and at the start of the Holocene (15-10 ka cal. BP) and after an interlude marked by the formation of a palaeosol, were gradually covered owing to Holocene water level rise, peat growth and coastal-deltaic sedimentation. Along the swamp and fen rimmed dune flanks, local peat formation often could keep up with the water level rise. This has created particularly favourable sites to collect age-depth data series that span several meters of elevation difference at a single location, while still meeting the condition that the sampled peat bed is on the relatively compaction-free substrate (Figure 3b). For this reason many inland dunes have been sampled to reconstruct past water levels (Jelgersma, 1961; Van de Plassche, 1982; Törnqvist et al., 1998; Berendsen et al., 2007; Van de Plassche et al., 2010). Especially the outer flanks of the highest dunes in inland dune complexes are suitable for sampling. In lagoon and lower deltaic settings, a subset of these dune flank samples can be upgraded from a GWL-related to MSL-related indicative meaning (Van de Plassche, 1982; Van de Plassche et al., 2005, 2010; Hijma and Cohen, 2019). Sampling bases of basal peat from near the base of the dunes, where the flanks are less steep and base topography becomes uneven, results in age-depth data points less suitable for relating to MSL. Such locations provide ULDs that with further analysis often proof to be perched above contemporary basal peat GWL of the surrounding floodplain.

Besides dated peat samples from inland dune flanks, the HOSLEA-NL data set contains 22 non-basal peat ^{14}C-dated charcoal ULD entries that also come from dune flanks. They are from swamp rim archaeological beds at the location where these intersected elevation contours of inland dunes (Van der Woude, 1983; Verbruggen, 1992). The archaeological bed surface is overlain by peat, marking the paludification of the area. The charcoal dates from just underneath constrain the timing of this, thus providing a GWL age-depth point.

3.3.4 Data points from peat beds on palaeo-valley floodplain surfaces

Section 2 introduced palaeovalleys as low elevated corridor areas with relative early and extensive basal peat growth and as gateways to further transgression (Figure 1a; Figure 3a). Their substrate consists of terraced fluvial sands, topped by a consolidated sandy clay floodplain unit that bears a developed palaeosol (Rhine-Meuse palaeovalley, widespread: Wijchen Member cf. Törnqvist et al., 1994; Autin, 2008; Overijsselse Vecht palaeovalley, more locally: Singraven Member). Basal peat overlying the floodplain surface associates to a river-flooding hydrological regime, characterized by eutrophic conditions and abundant reed, wood and fen-woody peat types (Bos et al., 2012). The pre-consolidated state of the underlying floodplain deposits at the time the peat formed, as marked by the palaeosol features, makes it a relatively compaction-free substrate, giving it a similar vertical accuracy as for basal peat index points from inland dunes and cover sand (Cohen, 2005; Koster et

al., 2017). Basal peat formed most extensively in relatively distal parts of the palaeovalley, i.e., in areas flooding regularly but receiving relatively little flood sediment. Peat started forming when downstream sea-level rise initiated rising floodplain

345   groundwater tables to just above the palaeosol surface, transforming floodplains into year-round moist flood basins, with the ground water tables and their gradient coinciding with mean-annual river water levels (Van Dijk et al., 1991; Kiden et al., 2002; Cohen, 2005; Koster et al., 2017). Along the rims of the palaeovalleys, GWLs indicated by basal peats can be more perched due to local seepage hydrological conditions (Cohen, 2005; Bos et al., 2012). The river gradient and seepage overprints make that those base basal peat data points cannot be related to MSL, and provide for inland GWL age-depth points only, in

350   some cases plotting meters above the contemporary sea level (Cohen, 2005; Koster et al., 2017; Hijma and Cohen, 2019). Data points evidently affected by these overprints are classified as secondary ULD types (ULD river gradient; Fig. 2), based on age-depth position comparisons with contemporary index points from downstream sites.

Top basal peat age-depth points from palaeo-valley settings do not suffer from these river gradient effects and have stronger

355   relevance for sea-level reconstruction. Where the peat is non-erosively overlain by fluvial-tidal (Rhine-Meuse palaeovalley) or fully tidal deposits (Overijsselse Vecht palaeovalley), the age of the top of the peat indicates the time of flooding by the sea and thus yields a SLIP (Hijma and Cohen, 2019). This is the case in the seaward parts of the palaeo-valleys from where the river valley turned into an estuary. Here transgression commenced relatively early and rapid and eventual inundation was many meters deep under brackish tidal open water regimes (Figure 1; Figure 3a).

360

3.3.5 Data points from peat beds on cover sand relief

Outside the palaeo-valleys, basal peat is predominantly encountered overlying coversand relief (Figure 3c). This buried surface often contains a developed podzolic palaeosol in the aeolian sand, indicating regionally low groundwater table positions during and after aeolian deposition (up to 12 ka cal. BP) and prior to basal peat formation (gradually after 9.2 ka cal. BP; Fig. 2b).

365   Basal peat on coversand often features a transitional contact from palaeosol organics (peaty sand) to the actual peat bed, regarded to be a result of relatively gradual drowning (Van de Plassche, 1982; Cohen, 2005), similar to the signal in floodplains and along inland dune bases in the palaeo-valleys. Base basal peat samples from coversand terrain contain ULD, especially when obtained from along flanks of subdued dune relief (Sect. 3.3.3). Again, top basal peat samples form potential SLIPs, provided that the top is non-erosively overlain by tidal sediments and that the thickness of the peat layer is limited.

370

In contrast to the eutrophic swampy basal peat on floodplain deposits and inland dunes in palaeovalleys, where the vicinity of flooding rivers brings nutrients, the peat overlying coversand often has a mesotrophic composition (sedge peat types). This is indicative for seepage-dominated hydrological regimes and explains the relatively perched positions of coversand basal peat data points, compared to nearby contemporary palaeo-valley data sets (Van de Plassche, 1982; Cohen, 2005). The degree of

375   seepage evidence strongly echoes local coversand topography (Bos et al., 2012). Base basal peat dates from relative lows in

the coversand terrain tend to return relatively old dates, in which case they are regarded as influenced by local hydrological conditions. In the database these samples are categorized accordingly as ULD local GWL. Mesotrophic peat over coversand also dominates- the lagoonal and tidal marsh fringing peat land that formed since 5.0 ka cal. BP (Fig. 2d) north of the Rhine-Meuse delta in the east-central Netherlands along the edges of the ice-pushed ridges and the Drenthe plateau, which are both source areas for regional seepage.
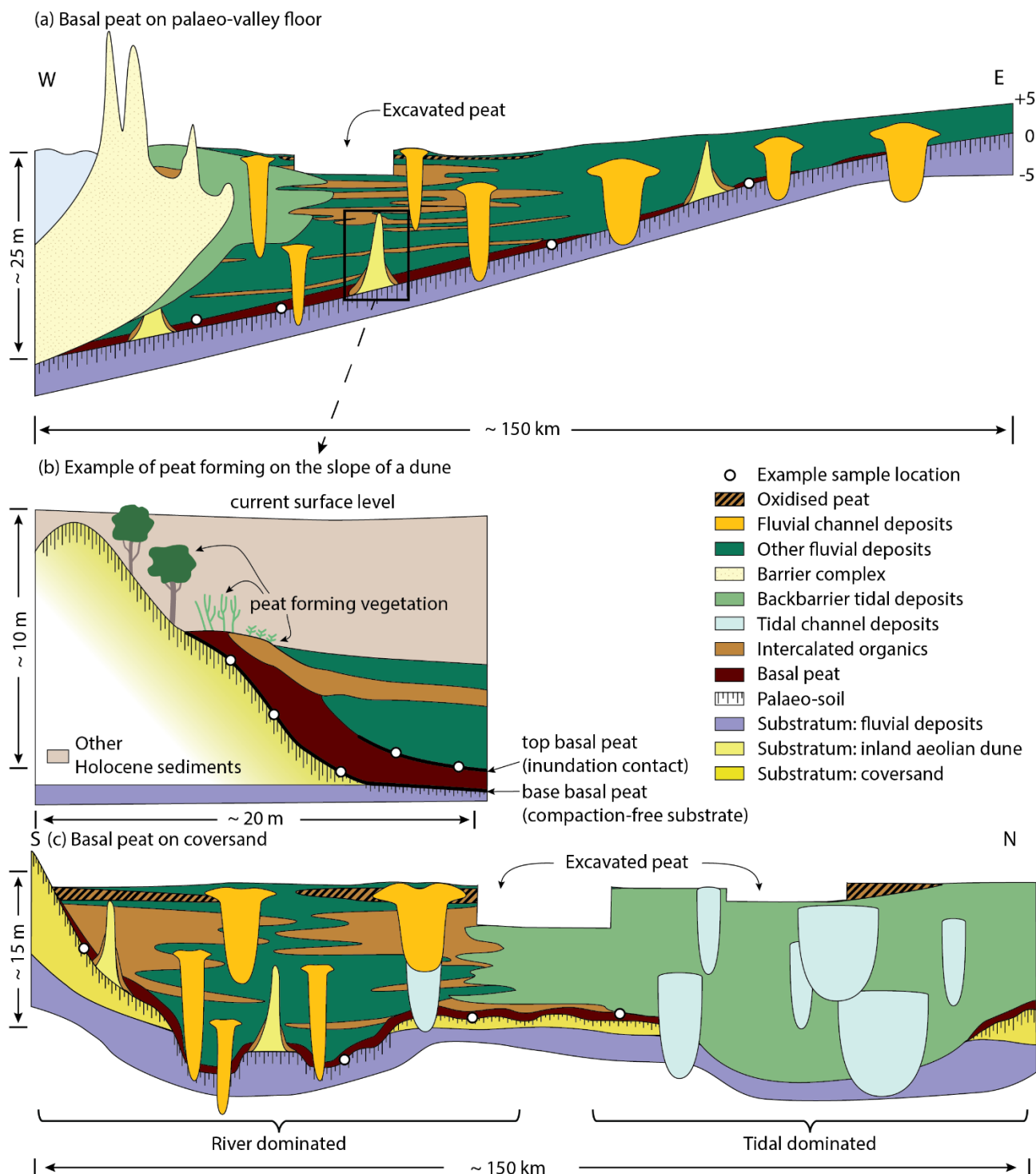
Figure 3 Examples of different sedimentary locations of basal peat layers: (a) On the floor of a palaeo-valley, (b) Along the flank of a river dune, (c) On top of cover sand (adapted from Kiden et al. (2008) and Bos et al. (2012))

3.3.6 Non-basal peat geological sea-level data

385

Some additional sea-level markers are reported in the HOLSEA-NL data set, including a set of brackish molluscs (Cerastoderma) obtained at great depth at Velsen (Van Straaten, 1954), and a set of index points obtained from ^{14}C dates of in-viva shells (Scrobicularia plana; Cerastoderma edule) found in the top of tidal flat deposits underneath artificial dwelling mounds, or terps, in the northwest of the Netherlands (Vos and Nieuwhof, 2021). The older set from Velsen is used mainly as additional dating control to peat radiocarbon dates collected from the same excavation, which provide base basal peat and top basal peat data.

390

The younger set from the northwestern Netherlands is included as they supplement and cross-validate basal peat data in the younger period (3000-1800 years cal. BP) for which basal peat data is sparser (Sect. 2). The levels with the Scrobicularia plana shells are located just below the transition between tidal-flat and salt-marsh deposits. The vertical position of this transition is regarded to mark the past MHW, giving the shells an indicative meaning of MHW − 0.33 m (Scrobicularia plana) or MHW – 0.4 m (Cerastoderma) (Vos and Gerrets, 2005; Vis et al., 2015; Vos and Nieuwhof, 2021). Calibrated ages for these samples are obtained using a marine calibration curve (Marine20; Heaton et al., 2020), and are corroborated with archeological dates from the overlying mounds.

395

4. Age-depth positions and evaluation

400

Where Sect. 2 and 3 are restricted to data intake, setting diversity (local and regional) and overall classification goals (ULD vs. SLIP), Sect. 4 describes further processing of the data in the HOLSEA-NL workbook. This comprises a series of adjustments regarding the vertical position of an indicator, starting from the originally reported sample elevation and indicative meaning, incorporating further compiled information. This step essentially reproduces earlier similar applications on subsets of the dataset (Kiden et al., 2002; Berendsen et al., 2007; Hijma and Cohen, 2010, 2019; Van de Plassche et al., 2010; Hijma et al., 2015), more uniform and over the entire HOLSEA-NL data set. HOLSEA-standard fields were used to transparently register this and expanded where needed – also to allow to omit or substitute specific corrections in future usage. Addressing the vertical corrections component-by-component serves this purpose. In many cases, the applied adjustments reproduce those from previous studies within a few cm, the difference owing to unification. This extends to acceptance/rejection and ULD/SLIP-usage decisions per data point, based on the age-depth data, indicative meanings and reliability judgements (e.g. Van de Plassche, 1982, fig. 4).

405

410

Importantly, the HOLSEA-NL data set includes all adjustment specifications also for originally demoted/rejected samples so that each decision can be re-evaluated per sample. Additional annotations on this are in note fields. This extension of the HOLSEA workbook improves the usability of workbook and data set and is of particular relevance when evaluating the type of indicator a sample represents. For example, only the RSL value of SLIP-samples includes the vertical adjustment for tidal

415

amplitude to plot palaeo-MSL, while the palaeo-MHW is provided for all samples that are graded to the palaeo-MHW. Otherwise only the standard palaeo-GWL is documented. Documenting the palaeo-GWL enables the use of the dataset for relative water-level rise reconstructions throughout the Holocene coastal plain and its subsectors, and for spatial-temporal

420 analysis (e.g., sea-level history, subsidence regime, accommodation attribution, coastal prism architecture).

4.1 Vertical corrections

Vertical positions are specified and accounted for through (i) original sample depth + uncertainty, (ii) offset calculations to get from sample depth to palaeo-water level depth, typically expressing GWL (Sect. 3); followed by (iii) further offset calculations to correct for compaction (upgrading depths), include palaeo-tides (upgrading to MSL expression) and corrections for two

425 types of subsidence (upgrading depths) and (iv) error propagations associated to all of this. Figure 4 below shows the full set of components considered, and the order in which correcting vertical offsets are applied and evaluated. For all datapoints several concurrent palaeo-water-level elevations can be calculated as shown in Figure 4 and Figure 5. The systematic processing chain facilitates iterative evaluation and switching between ULD and SLIP indicator type status (former GWL/MHW resp. MSL expression).

430

Decompaction (a vertical offset + uncertainty) is a correction that is always considered. Palaeo-tidal considerations are relevant to all data points that are classified as SLIPs, and the user may either use the provided values (expansion of standard HOLSEA protocol; Hijma and Cohen, 2010, 2019) or fall back to using the modern tidal range in the region. The correction for background basin subsidence we regard optional to include. It is typically required (e.g. Kiden et al., 2002; Vink et al., 2007)

435 if a comparison with GIA models is sought, though it is typically skipped (Hijma and Cohen, 2010, 2019; e.g. Van de Plassche et al., 2010) in traditional relative sea-level curve construction plotting. The correction for so-called deep anthropogenic subsidence applies to specific subareas in the NE Netherlands that have been subject to 20-21st century gas extraction and can be regarded as a sample depth correction (up to 0.4m) to apply in most use cases. Below further details are given on these critical corrections.

440 **4.1.1 Decompaction**

Decompaction corrections can refer to the correction of two processes: (i) post-depositional compaction of the beds directly underlying the sample, which is mostly relevant for top-of-basal peat samples and can be up to 5 m and (ii) to the self-compaction of the sampled material. This is a smaller component, but it applies to all peat samples, the correction averaging 0.06 m. The post-depositional compaction is corrected for using the depth to the consolidated substrate (m) (Field 18 in

445 supplementary HOLSEA workbook) and a decompaction factor. The decompaction factor depends on the overburden thickness, with peat beds deeper below the surface experiencing more compaction than the shallower peat beds. For samples taken deeper than 20 m below the surface (x = 21) a decompaction factor of 3 is used. A decompaction factor of 2 is used for samples shallower than 2 m below the surface (x = 130). For all other samples in between 2 and 20 m a decompaction factor

of 2.5 m is used. This is documented as the compaction correction (m) (Field 64) in the HOLSEA workbook. In specific cases from reclaimed land the decompaction could be underestimated, since the current overburden thickness is lower than before reclamation, which is currently not accounted for. The associated uncertainty is compaction correction dependent (Field 65). The compaction correction uncertainty considers an error margin of 0.02 m for the depth to consolidated surface and assumes an uncertainty of 0.5 in the decompaction factor. Thus, for a sample with a midpoint 0.10 m above the consolidated substrate and taken 8 m below the surface, the decompacted midpoint is 0.25±0.07 m above this substrate.

For the sample thickness (Field 21) a decompaction factor of 2.5 is applied around the sample midpoint, consistent with investigations in Van Asselen (2011) and past usage in Hijma and Cohen (2019). The sample decompaction uncertainty (Field 24; 'Sample thickness uncertainty (m)') is set to half the decompacted sample thickness. This is a modification of earlier decompaction approaches by Berendsen et al. (2007) and Van de Plassche et al. (2010) who used a decompaction factor of 2.5 for the bases of their sampled beds and 3.5 for their tops, accounting for both the compaction of the underlying unconsolidated sediment as well as the compaction of the sample itself. In the HOLSEA format these two components are split into separate steps, which is why a single decompaction factor was used to correct the sample thickness relative to the mid-point and a separate decompaction factor for the compacting the underlying unconsolidated sediments. This also allows to account for the larger variations in sample depths which are encountered in the HOLSEA-NL data, compared to the smaller variations in depths in the studies of by Berendsen et al. (2007) and Van de Plassche et al. (2010), which focused on specific sites.

4.1.2 Past tidal amplitude and flood-basin effect

A tidal amplitude is required to calculate the vertical positions of SLIPs that expresses MSL. This counts for data points that have a RWL = GWL = MHW assigned indicative meaning (Sect. 3.3.2). The tidal amplitude (half the tidal range) is the offset between MHW and MSL and unlike all other vertical corrections considers a downward vertical correction (Fig. 4 and 5). Modern tidal ranges along the Dutch coastline are controlled by the North Sea bathymetry and its connection to the ocean global tides. Recent developments of these tidal ranges are known from centuries of observations and are regarded to be relatively stable. These values are considered to have established when global sea levels reached their high stand and the North Sea approached its modern depths, around 6800 years ago (Van der Molen and De Swart, 2001). Over the duration of the full Holocene, however, the tidal ranges are considered time variant, especially for the period from 9000 to 6800 years ago when the southern North Sea was inundating, shallow bathymetries deepened, and coastline positions shifted. To allow for this, rather than to use modern tidal amplitudes (HOLSEA standard), we implemented a lookup scheme for palaeo-tidal amplitudes in the HOLSEA-NL set (available from earlier model-reconstruction work; Van der Molen and De Swart, 2001; Uehara et al., 2006; Ward et al., 2016), and used those for the tidal corrections. Herein we geographically expanded an earlier application by Hijma & Cohen (2010, 2019). Similar, to the latter work we continued with specifying the palaeo-tidal amplitudes (pMHW) as meta-information in note fields in the HOLSEA workbook. This considers MHW (pMHW) in the near shore just seaward of the modern coastline.

Nearshore tidal amplitudes propagate inland and are deformed into estuarine, fluvial-tidal, and lagoonal waters inshore, to which the peat forming hydrological systems originally graded. In the wide, underfilled, estuarine back-barrier lagoonal-deltaic and lagoonal situations of 9000-5000 years ago (Fig. 1), inland tidal dampening is regarded to have occurred in SLIP producing areas (Hijma & Cohen, 2019). This inland lowering of water tables to a level in between seaward MHW and MSL, is called the flood-basin effect (FBE), and occurs especially where the semi-diurnal tidal wave travels through a narrow bottleneck in and out of broader flood basins inland (Van Veen, 1950; Zonneveld, 1960; Van Veen et al., 2005). To correct for this, in addition to the pMHW geographic lookup scheme, an FBE-factor is specified.

Various studies have assessed past FBE in RSL-reconstructions, in particular in the lower Rhine-Meuse area and the Flevo-lagoon region (Van de Plassche, 1982, 1995; Berendsen et al., 2007; Van de Plassche et al., 2010; Vis et al., 2015; Hijma and Cohen, 2019), by cross-comparison of age-depth plots for relative seaward, central and inland subsites. This way, the sites where GWL age-depth data plot youngest-deepest can be identified and from this it is inferred that the flood-basin effect must have been largest at these sites. These youngest-deepest points are promoted to SLIP status (possible to calculate MSL positions) while leaving surrounding contemporary sites as ULD (expressing GWL positions only). Assessment whether flood-basin effect was intermediate (some dampening) or maximally developed (full dampening) requires cross-checks with palaeogeographical reconstructions. Hijma and Cohen (2019) did the latter for the lower Rhine-Meuse delta leading to a prescription of past FBE as intermediate (50% dampened, FBE = 0.5) in the relative open situation before 7.5 ka, FBE = 0.75 between 7.5 and 6.5 ka, and full dampening FBE = 1 established 6.5-3.0 ka. For the other regions, FBE corrections for data points classified as SLIP were newly assessed, based on the HOLSEA-NL data coverage, with cross-checks against available palaeogeographical reconstructions (Vos et al., 2018; panels in Fig. 2 and additional), especially in the Flevo lagoon and northern regions. For the western coastline, North Holland to Zeeland, we prescribe the same tidal dampening regime as used by Hijma and Cohen (2019) for the lower Rhine-Meuse delta. For the Waddenzee region tidal dampening is assumed to play a less dominant role. The indicators from the western Waddenzee are assigned no flood-basin effect, since no large flood basins formed around the SLIP producing samples. The eastern Waddenzee region is expected to have had some tidal dampening during the Middle Holocene, but this effect decreased towards the Late Holocene. Therefore, before 7 ka the tide is 50% dampened (FBE = 0.5), between 7 and 5 ka this decreases to 25% dampening (FBE = 0.25) and after 5 ka we assume no dampening.

We note that the prescription of FBE only applies to the SLIP producing locations (as in Hijma and Cohen, 2019). If the mentioned FBE values are applied to nearby contemporary ULD, it results in 'falsely' shallower MSL positions than at the SLIP locations. The GWL at ULD locations surrounding SLIP locations, is to be regarded more strongly pMHW-controlled towards the sea and more strongly river-gradient or otherwise terrestrial hydrologically controlled inland, but the database does not quantify how strongly. The FBE correction factor is registered together with the pMHW value, in the note field.

4.1.3 Background basin subsidence

Because the coastal plain of the Netherlands overlies the long-term sinking North Sea sedimentary basin, it should be considered that part of the relative water level rise documented by the dataset is due to tectonic and sedimentary loading subsidence. Therefore, optionally, depending on application, (see above) the effect of this background term is removed by 520 applying a vertical correction. As input to this correction, a map product specifying a background rate was used, as done in Cohen et al. (2021: their Vertical Land Motion) for a Last Interglacial sea-level database, with values similar to those in use for the region since Kooi et al. (1998). For each sample location, values were read and multiplied with the age of the sample, and uncertainty on age plus rate propagated accordingly. The HOLSEA data workbook stores this under "Tectonic correction (m)" (Field 66) and "Tectonic correction uncertainty (m)" (Field 67).

525

The upward corrections range from 0 up to 1 m in the onshore part of the study area, with uncertainties between 0.01 and 0.18 m. The range reproduces earlier quantification of a background subsidence term in relative sea-level data in Kiden et al. (2002), Vink et al. (2007) and Simon and Riva (2020). Within the study area rates are highest in the northwest part of the study area. Averaged values listed for offsets considered for SLIPs plotted in Fig. 2b (9.2-6.6 ka cal. BP) serve as an example: Rhine-
530 Meuse palaeovalley 0.5 m; Vecht palaeovalley 0.8 m; inland Flevo-lagoon 0.6 m; NE Wadden Sea 0.3 m.
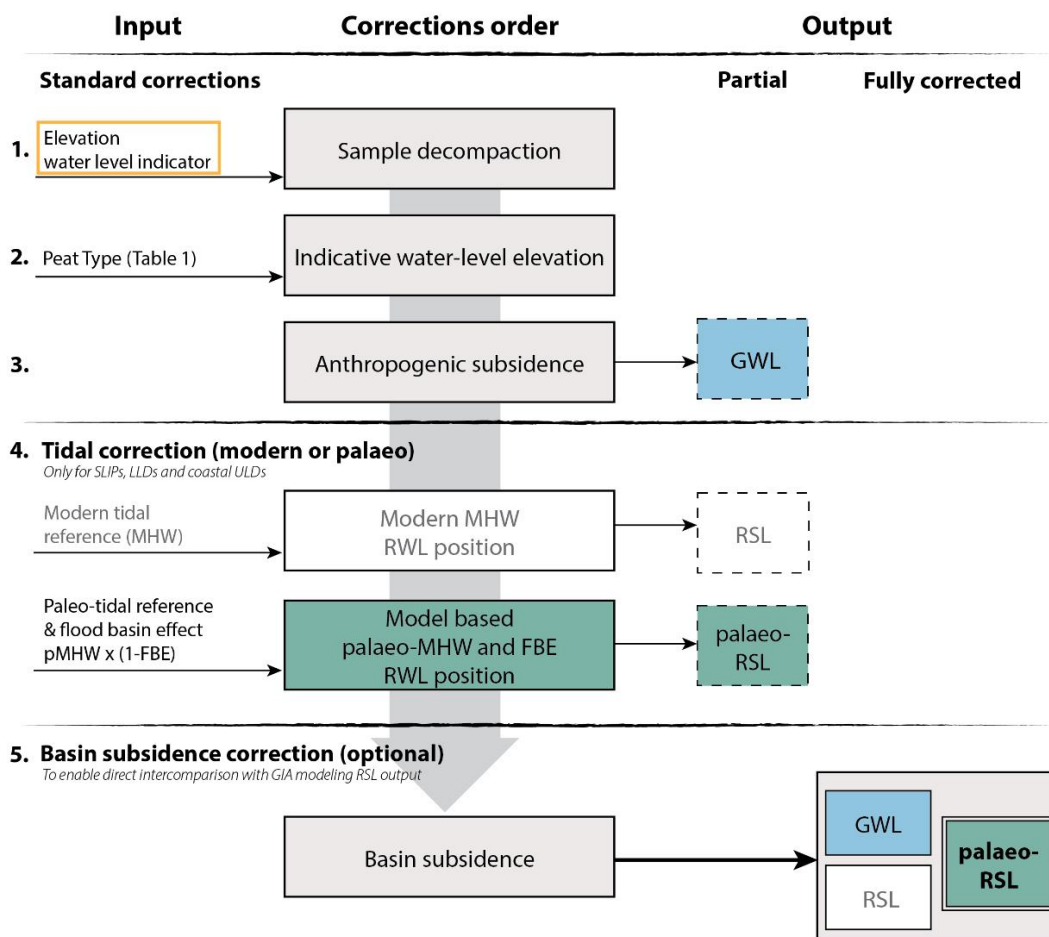
Figure 4 Flowchart of water level indicator sample processing chain. The final fully corrected output is a basin subsidence corrected palaeo-RSL value.

535 **4.1.4 Anthropogenic deep subsidence**

The extraction of resources such as gas, water and salt from a range of depths well below the basal peats, has caused significant recent subsidence in specific areas of the Netherlands (e.g. NAM, 2017, 2020). This subsidence has influenced the depth of Holocene water level indicators and an upward vertical correction is required to remove unwanted lowering of palaeo-water level indicators and correct joint plotting of samples collected 'in 1950-60ies', 'in 1990s' and 'in 2010s' from these human-

540 induced subsidence affected areas. This upward correction is dependent on the year of coring: larger for more recent years, and specified in the subsidence history maps by NAM (2017, 2020). In the strongest affected areas this correction is up to 0.36 ± 0.10 m. The HOLSEA workbook records this separately as "Human-induced subsidence (m)" (Field 68) and "Human-induced subsidence uncertainty (m)" (Field 69).
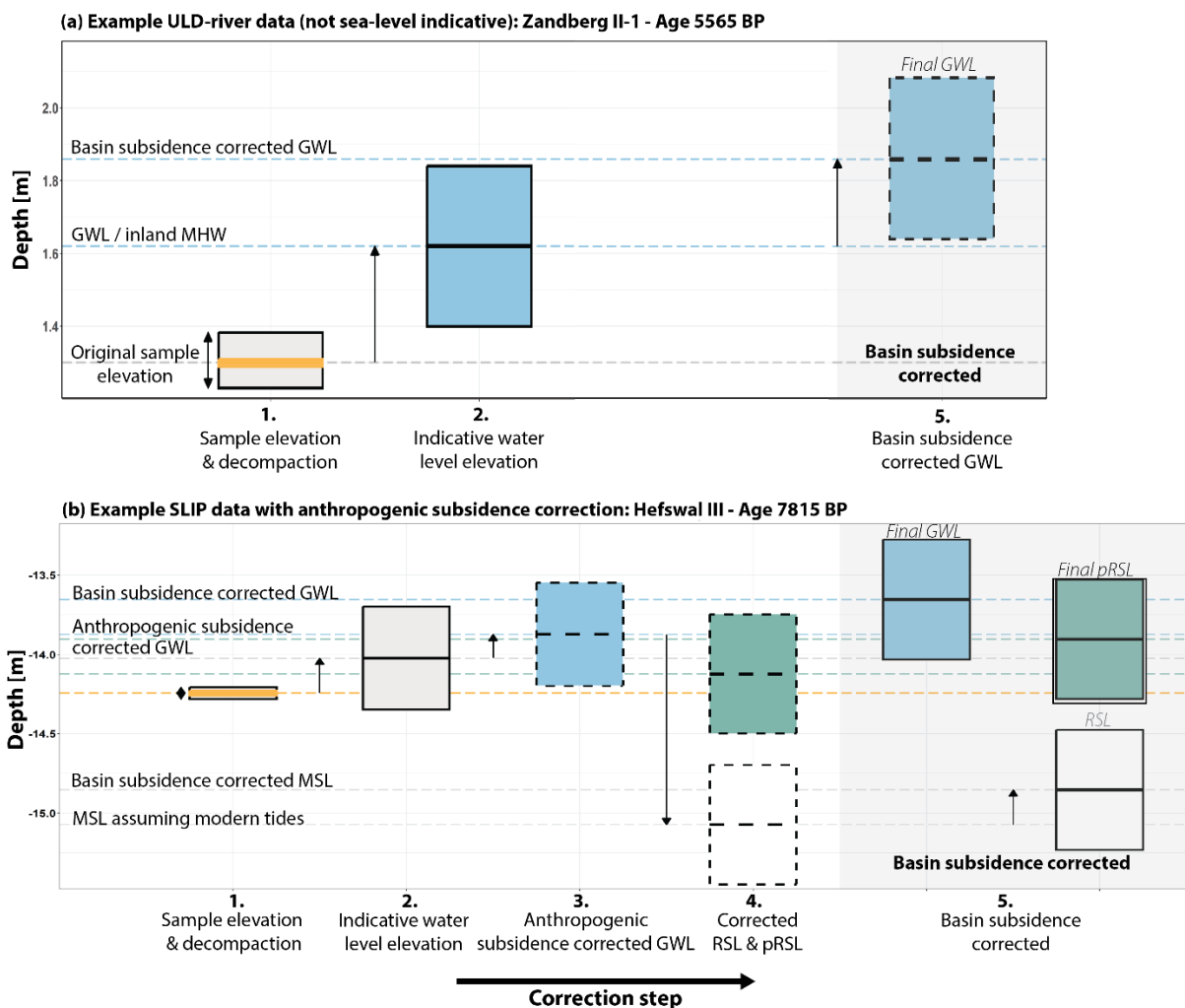
Figure 5 Dashboard of sample elevations of two example samples for visual inspection of vertical positioning owing to vertical correction steps. (a) Inland GWL / Upper limiting sample without anthropogenic subsidence, (b) Fen peat SLIP sample from the northeast of the Netherlands, affected by deep anthropogenic subsidence

The application of the vertical corrections generally results in an upward shift of the final GWL or final RSL (pRSL in Figure 5) elevation with respect to the original sample elevation (Figure 5). On average, the final RSL elevation of basal SLIPs is 0.4 m higher than the original sample elevation. For intercalated SLIPs the difference much higher (~1.5 m) due to the larger upward correction. The tidal correction influences the elevation of the sample strongly. Figure 5 shows that assuming modern tides instead of using a palaeotidal model results in much lower RSL elevations, ~0.2 m below the original sample elevation. For Middle Holocene SLIPs, using a palaeotidal model causes an average upward shift of ~0.7 m, because of the gradually increasing tidal range and tidal dampening. This shift is also present in Late Holocene SLIPs from areas with strong tidal damping, whilst in areas the without tidal damping the Late Holocene MHW is equivalent to modern MHW.

4.2 Dating information, including calibration

Radiocarbon dating has been used to determine the age of all the samples. Because many datapoints were previously published and assigned various "unique sample IDs" we decided to use the lab code provided for dating as Unique sample ID (Field 1), to avoid confusion over the numbering system. Conform the HOLSEA workbook, sample ID (Lab-number), dating result (age
560 + uncertainty, in ^{14}C BP) are the primary dating information. Where available, δ^{13}C (in ‰) are provided and source reference of the date is provided as meta-information (see also Hijma et al., 2015; Hijma and Cohen, 2019). For very early radiocarbon dates, measured before 1962 (original Gro-numbers from the Groningen lab) a later published correction for the Suess effect has been applied, following Vogel and Waterbolk (1963). These samples are documented in the HOLSEA-NL workbook using their converted GrN-number, with the original ^{14}C-age document in the notes. Additionally, a bulk error is provided for sample
565 dated using conventional dating (e.g., GrN-numbers), except when explicitly stated that it was not a bulk sample (e.g., piece of wood). The bulk error is provided in the radiocarbon tab and a note is made in the sampled material.

The ^{14}C-dating results from terrestrial material such as basal peat macrofossils and charcoal, have been calibrated using the atmospheric calibration curve IntCal20 (Reimer et al. 2020). We recalibrated older samples. Note that dating results earlier
570 calibrated with IntCal04 and IntCal13 (in source literature) hardly differ from the IntCal20 recalibration (in HOLSEA-NL), as all our data is from within the Holocene part of the calibration curves.

4.2.1 Bayesian calibration

Besides individual date calibrations ('unmodelled' calibrated ages), the workbook provides a second set of fields storing Bayesian calibration results for vertical series of samples from the same site, as advocated for in Cohen (2005) and Hijma &
575 Cohen (2019). The 'modelled' calibrated ages were generated running CQL scripts in the OxCal 4.4 software (Bronk Ramsey, 2008, 2009) partly reused from Cohen (2003) and Hijma & Cohen (2019). The sequential calibration model further narrows down the calibrated age of some samples, decreasing the age range by 10 up to 500 years. The decrease in age range is generally larger when conventional dating was used (mostly dated before 2000), compared to those dated using AMS-dating.

5. Processed data overview

580 This section aims to summarize the dataset contents in its full processed form, highlighting the new achieved uniform coverage. The focus is on describing systematic spatial differences and on showing the quantitative effects of including regarded optional vertical corrections. To do so, the data is grouped in seven regions (Figure 6), that are also Holocene-geologically different. The boundaries between coastal subregions follow Pleistocene drainage divides (Vos et al., 2011, 2018; Cohen et al., 2017). The Rhine-Meuse and Vecht palaeovalley are further west-east subdivided based on dominance of coastal-and/or-tidal
585 (seaward) vs. fluvial-and/or-peaty Holocene depositional circumstances (landward) (Figure 2).
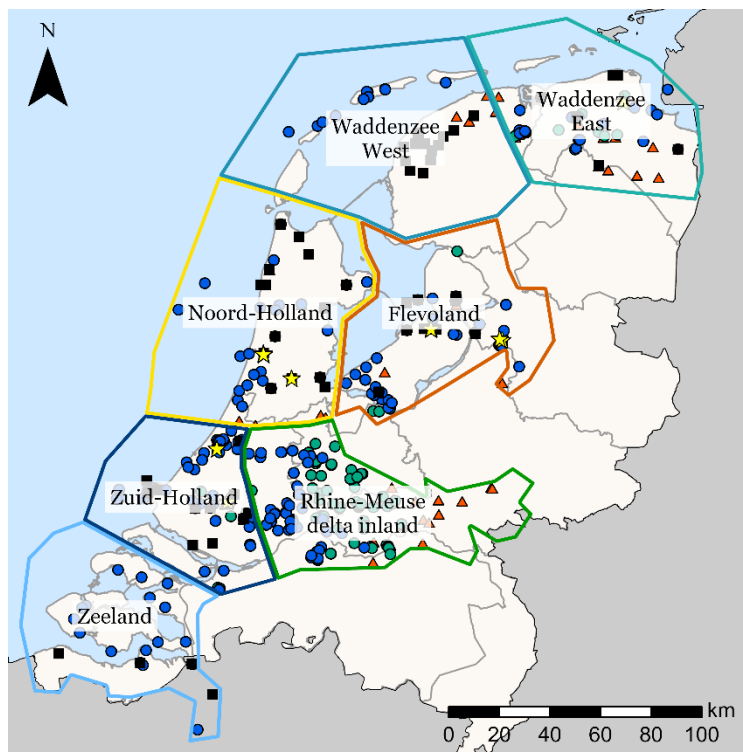
Figure 6 Overview map of water-level indicators and region divisions. Multiple indicator points from the same location are plotted on top of each other.

5.1 Spatial distribution

590 The HOLSEA-NL data set contains 681 water-level indicators, of which 121 SLIPs, 14 LLD points, 367 primary ULD points, 129 river-gradient affected ULD and 50 local-GWL secondary inland ULD data points. Most of the collected data is from the Middle Holocene (between 8.2 and 4.2 ka BP; Figure 7a), because of three main reasons. First, this period corresponds with the inundation of the Pleistocene surface in large parts of the Netherlands during the Middle Holocene, due to which large-scale peat growth was possible throughout the coastal areas of the Netherlands (Vos, 2015). In this period most of the basal

595 peat layers were formed (Figure 2b, c). It can be seen in Figure 7.a that the local GWL indicators are the oldest indicators, some dating back to the Late-Glacial. In this period peat formed only locally in the research area because the sea-level was not high enough to reach above the Pleistocene surface. Older basal peats linked to RSLR are found offshore, outside the study area, where the Pleistocene topography had a lower elevation resulting in an earlier inundation. Conversely, the youngest basal peat samples are found further inland or on top of Pleistocene covers sand and river dunes. Second, erosion has caused the

600 basal peat to disappear in areas along the coast and near rivers. This has resulted in the disappearance of many younger peat layers. And third, in addition to natural erosion, human activity has resulted in the removal of large amounts of peat from the subsurface (Vos, 2015). Large-scale peat excavations have occurred since the Middle Ages when peat was mined extensively (Pierik et al., 2017). Additionally, embankments of rivers and artificial drainage led to oxidation of peaty top soils. The result

is that large parts of the shallower peat layers in the Netherlands have disappeared, including some of the younger and shallower

605 basal peat layers. Therefore, water level reconstructions of the Late Holocene require additional methods and indicator types

other than basal-peat samples.
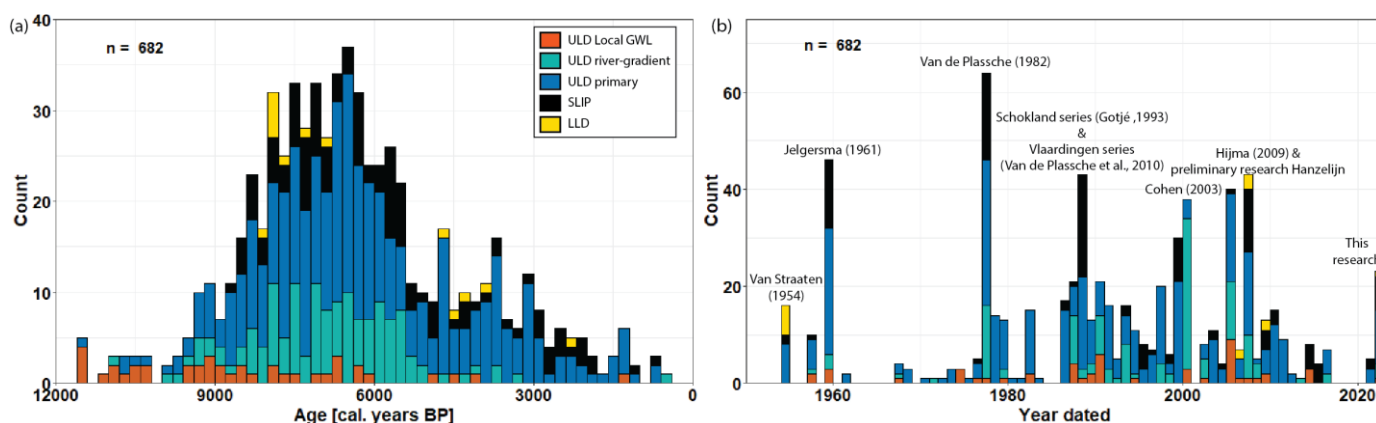
Figure 7 (a) Distribution of the number of water level indicators by age from 12 to 0 ky cal. BP; (b) Distribution of water level indicators sorted by the year the samples were dated. Some large sampling campaigns are indicated. Rejected data is omitted.

610 Figure 7b shows when the indicators were dated and serves as an illustration of the diverse, stepped research history behind

the database contents. Many of the samples were collected and dated in large campaigns, some of which are noted in de Figure

7b. From the '80s onwards, smaller sets (single sites) were collected, and the nature of the producing studies diversified. Since

2000, routine sampling as part of archaeological prospection attached to infrastructural projects (e.g., Hanzelijn railroad

through Flevoland) has become an important supplier. The 2022/23 spike includes new obtained dates from the North Holland-

615 Flevoland fringe region collected as part of the present research, while compiling the database (see also Sect. 5.2).

When dividing the data over the regions, some distinction in year of dating is visible between the different regions. This

variation shows in part the shifts in focus for water-, and sea-level research in the Netherlands. For example, in Noord-Holland

most samples were dated already between 1955 and 1960 by Van Straaten (1954) and Jelgersma (1961), with very limited

620 additional samples. We tried to fill this gap with new submissions in 2022-2023. On the other hand, from Flevoland most of

the samples are collected from 1989 onwards, starting with the samples collected by Roeleveld and Gotjé (1993) (published

in Gotjé (1993)). Figure 8 reveals the spatially uneven distribution of water level indicator collection, with the great majority

collected in the central part of the Netherlands (Zuid-Holland, Flevoland and Rhine-Meuse central). This is again strongly

linked to the research focus of past studies. For the northern areas the number of indicators is gradually increasing over the

625 past two decades, showing an increasing interest for GWL and RSL reconstruction in this area (Meijles et al., 2018; Quik et

al., 2021; Makaske and Maas, 2023). Especially for Zeeland in the southwest, collection of new data is very limited.
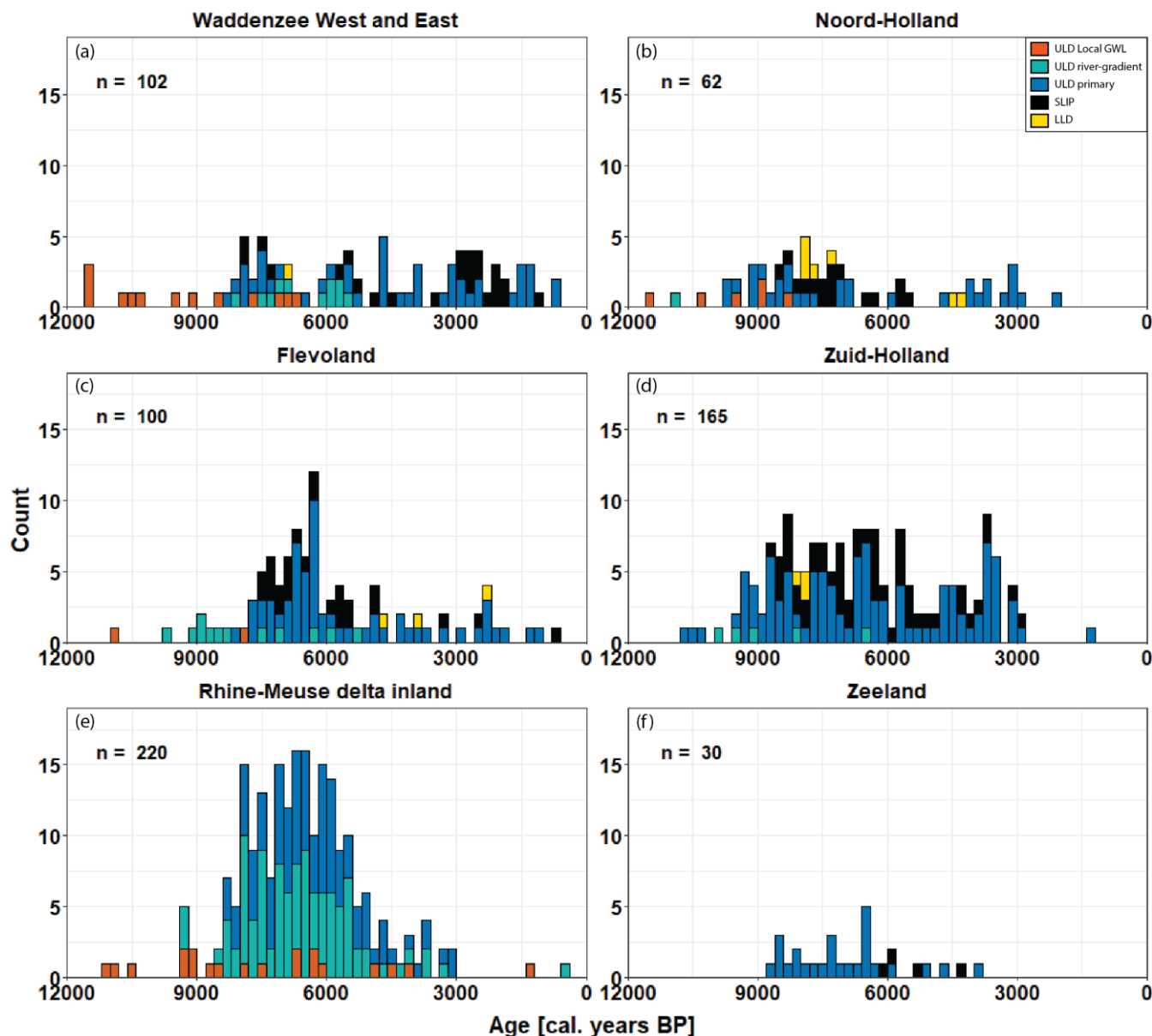
Figure 8 Distributions of water level indicators sorted per subregion by age from 12 to 0 ky cal. BP. Rejected data is omitted.

5.2 Age-depth plots

630   Separating the age-depth plots of the corrected water-level data (i.e., without palaeo-tidal correction) per region shows the spatial variability in the data (Figure 9). A consistent water-level rise trend is visible in the denser sampled regions Zuid-Holland, Rhine-Meuse delta inland, Flevoland and Waddenzee. In contrast, the plots from Noord-Holland and Zeeland show a patchier pattern, because of the lower number of indicators in these regions. Regarding temporal coverage: the coastal regions Zuid-Holland, Noord-Holland and the Waddenzee host relatively older ULD-tidal and SLIP data, starting ca. 9-8.5 ka cal.

635 years BP, while in the more inland regions Flevoland and Rhine-Meuse delta this commences ca. 8-7.5 cal. years BP. This reproduces and confirms earlier investigations of the transgression rate (e.g. Vos, 2015; Koster et al., 2017).

The setup of the HOLSEA-NL workbook allows for several variants of age-depth plotting, useful at different stages of evaluation and iterative classification (SLIP, ULD etc.) and for different derived data set use (see also Sect. 4.1). The data set

640 can be used to make customised age-depth plots using for instance original depth, inferred GWL position, further inferred MSL positions, or further background-subsidence corrected MSL positions (Figure 4 and Figure 5). Figure 10a-c provides three variants of indicator depth plotting against age, that can be zoomed into to evaluate clusters of apparent outlying data for possible under-, or overcorrection. To prevent misinterpretation of the different age-depth data, we recommend the use of explicit labelling and clear caption details.

645

Overall, SLIPs, ULD and LLD subsets each show relatively rapid water-level rise during the Middle Holocene (from ca. 9 ka onwards), which slows down towards the Late Holocene (semi-linear after 4 ka). The river gradient ULD echo this trend, but in higher positions, lifted up by the river gradient. It is also clear that the local GWL data does not follow the general curve but shows a more diverse pattern (Figure 10a). Figure 10a shows the elevation of all the water-level data through time with

650 corrections for compaction, background basin subsidence and anthropogenic deep subsidence, but without tidal corrections. Figure 10b shows the corrected water-level data (in grey) and the fully tidal corrected RSL data. The corrected water-level data shows a slight upwards shift compared to the un-corrected data. Also, the propagated uncertainty to the depth positions increases, especially for the older datapoints.

655 To illustrate what the databasing activity has added to the inventory – and how zoomed-in age-depth plot evaluations worked out, we highlight the data currently assembled for North Holland and Flevoland. North Holland has been a region where basal peat data was relative scarce (e.g. Van de Plassche, 1982; Koster et al., 2017), and Flevoland a region where basal peat data is of diverse origin (Schokland research efforts: Roeleveld and Gotjé, 1993; Van de Plassche, 1995; Almere research efforts: Makaske et al., 2003; various archaeological investigations 2000-2020s). To add to Middle Holocene data coverage, a cluster

660 of sites were dated from SE North Holland (Durgerdam, Slotermeer, Diemen: this research, N=12) and from within IJsselmeer (Van den Brenk et al., 2023; this research, N=5). To add to Late Holocene data coverage, dates from central Flevoland (Hanzelijn: Hamburg and Knippenberg, 2006; De Moor et al., 2009; N=16; Kampen-Cellemuiden, this research; N=5) were added to the existing data. To highlight some findings and actions:

- Inspection of the Flevoland data after initial entry revealed outlier clusters 5000 to 4000 years-old plotting 'too young,

665 too deep', that in databases were registered as 'basal peat' dates but in detailed reports (Van Lil, 2008; De Moor et al., 2009) had actually been identified as peat detritus: sediment from peat-lake bottoms, calved from fringing peat bodies, redeposited at lower elevation. These data points were demoted to LLD data points, and they are partly rejected as sea-level indicators (see Figure 9c).

- Inspection of the remaining (non-lake bottom) Hanzelijn and the Kampen-Cellemuiden data, allowed to identify
670   lowest-youngest ULD datapoints in the series and in three cases upgrade these to SLIP status for c. 3000, c. 2500 and
c 900 cal. yr. BP (Figure 9c), which supplement and confirm the non-basal peat terps SLIP set (see Sect. 3.3.5). The
eastern fringe of the Flevoland coastal plain is identified as a region holding MSL-reconstruction relevant peat
resources at relatively shallow position (within 1 meter below OD), more strongly and explicitly than in earlier
national compilations.
675   - Inspection of data from SE North Holland for location Slotermeer at 7500 cal. yr. BP, identified as a 'too young, too
deep' outlier cluster: presumably a Middle Holocene lake situation, similar to the Late Holocene 'Hanzelijn' example
mentioned above. These data points were demoted to LLD data points (see Figure 9b).

- Inspection of potential onset Late Holocene SLIPs from locality Schoorl in NW North Holland (4500-3500 cal yr BP,
(Ente et al., 1975)) suggests these to plot relatively low (Figure 9b), for which there are competing explanations:
680   tectonic correction (~0.45 m over 4000 yr) may be locally underestimated, tidal correction (0.8 m) overdone, or
compaction correction (0.15 m) underestimated. Because of the uncertainty in the vertical corrections and the low
elevation of the samples, these potential SLIPs were rejected. Additional sampling in this area and more detailed
research on the vertical corrections at this site will improve the age-depth reconstruction and helps identify why these
Schoorl points are plotting lower than surrounding points.

685

A selection of the SLIPs per region from the parent database can be used to fit relative sea-level curves per region (Figure
10c).

These curves will deviate back in time because of differential subsidence – N Netherlands curves being positioned below the
SW Netherlands curve for the period between 8.5 to 5 ka cal. BP. For sea-level markers of ca. 8000 years ago, data and curves
690   in Figure 10c suggest 2 to 4 m more subsidence to have occurred in the N Netherlands than in the SW. This is a similar finding
as earlier communicated – partly corroborating, partly reproducing, partly detailing – work by Kiden et al. (2002) and Vink et
al. (2007), who attribute the regional differences in the Netherlands to GIA subsidence terms.

More extensive comparison of the trends from different regions is recommended, for example, using Bayesian modelling for
the SLIP data like in Cahill et al. (2015). Narrower quantification of the GIA contribution and its decay from the Middle
695   Holocene (8000-4000 cal. yr. BP) to Late Holocene (last 4000 years) using the HOLSEA-NL database is part of ongoing
research. This type of research extends from geological data to incorporating modern tide gauge, GNSS and satellite sea-level
monitoring era data (e.g. Vermeersen et al., 2018; Steffelbauer et al., 2022) – beyond the scope of this dataset and paper that
restricts to geological water level data. Nevertheless, evaluating the sea-level rise and subsidence rates from both realms,
geological and modern, and integrated usage of the two resources is relevant when reconstructing the Late Holocene and recent
700   RSLR (Simon and Riva, 2020), and the HOLSEA-NL database contributes to iterating that.
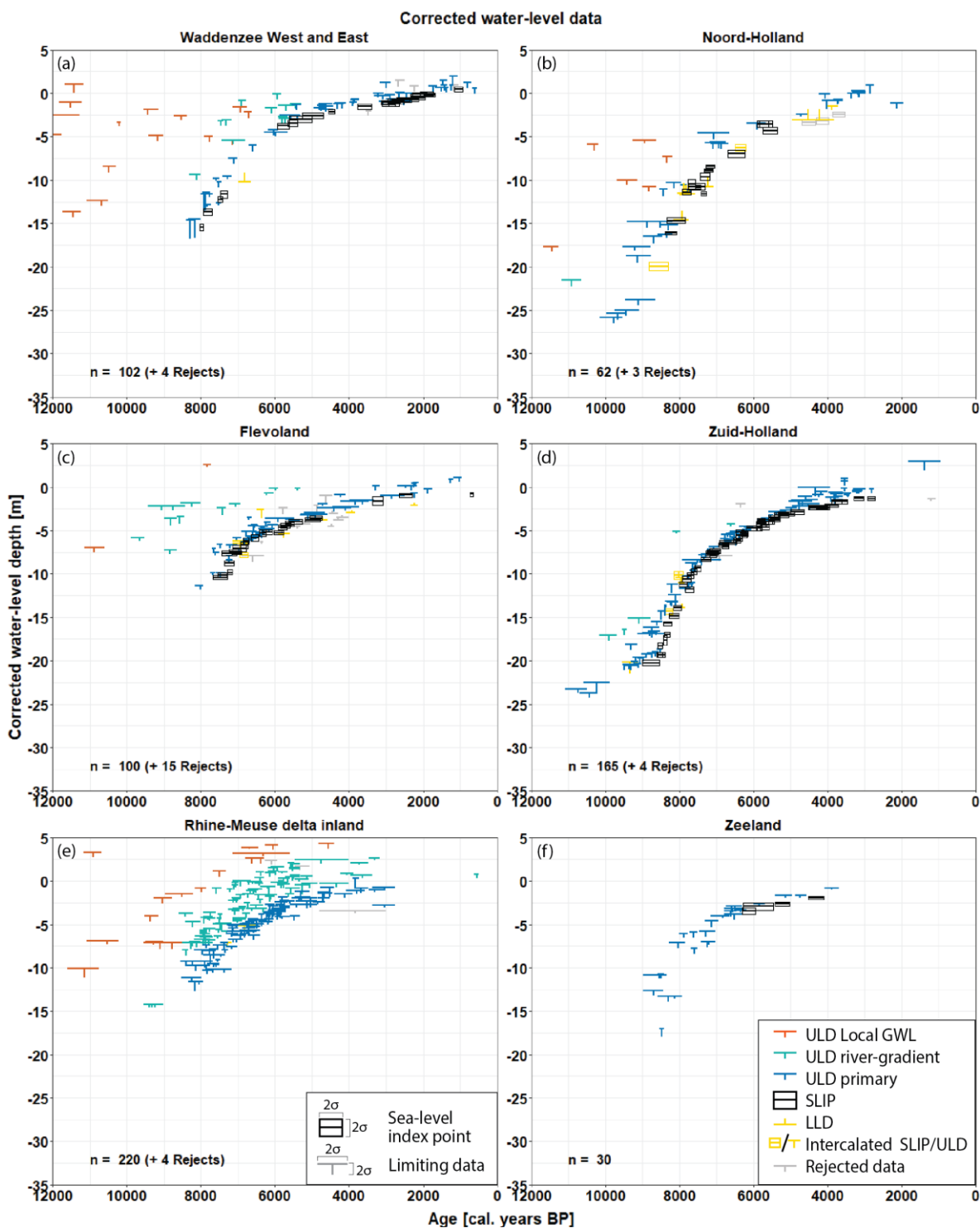
Figure 9 Age-depth plots of the corrected water level elevation for geological indicators per subregion from 12 to 0 ky cal. BP
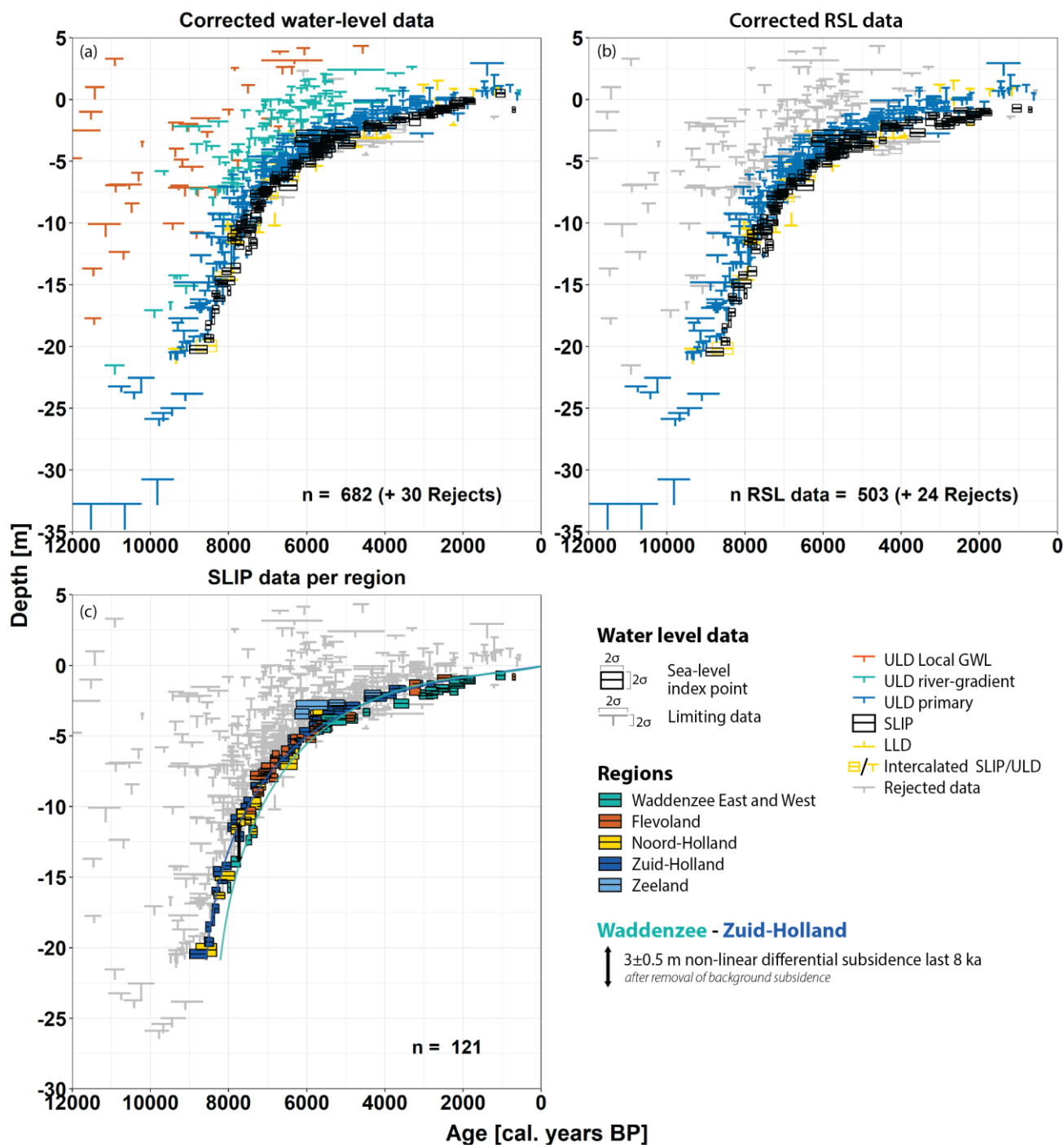
Figure 10 Age of indicator data plotted against various sample elevations based on different vertical adjustments applied: (a) Using the indicative water-level, and corrected for decompaction, background basin subsidence and anthropogenic deep subsidence; (b) As A but incorporating a palaeotidal correction for SLIPs and removing secondary ULD and rejected samples (both in grey); (c) Fully processed SLIP data (all vertical corrections considered), coloured by Region, with tentative curves for the Waddenzee (light blue) and Zuid-Holland SLIP data (dark blue) to illustrate deviation back in time.

6. Discussion

Bringing together water level indicator data shows the prospect of reconstructing relative water level rise on a larger spatial scale. Previously, water level or sea-level reconstructions were constrained locally to areas where there was a straightforward sampling opportunity (i.e. Zuid-Holland: 'Rotterdam', 'Lower RM-delta') and as this area was revisited several times, it resulted in a high data density (e.g. Jelgersma, 1961; Berendsen et al., 2007; Van de Plassche et al., 2010; Hijma and Cohen, 2019). Compilations for other regions were more incidentally executed (Jelgersma, 1961; Kiden et al., 2002; Makaske et al., 2003; Meijles et al., 2018). The newly compiled data set and explicit vertical correction bookkeeping first of all creates opportunity to cross-validate quality and accuracy of the dataset (Sect. 6.1). Furthermore, it allows for superregional water level reconstructions, in previously data sparse regions.

6.1 Uncertainties and limitations

In this paper and in the accompanying HOLSEA-NL data set, we attempted to document all Holocene (coastal) water level indicators for the Netherlands that are relevant for reconstructing relative groundwater rise, sea-level rise, and regional subsidence. Given the long history of water level and sea-level research in the Netherlands, a broad range of documentation of suitable data existed, not always easily accessible, from which in the future new details may emerge that could lead to updating/re-processing of individual entries. Furthermore, ongoing and future research is expected to generate further new water level indicator data and gradually increase the HOLSEA-NL data density. Therefore, the compiled data set of water level indicators and their accompanying metadata, should be viewed as a living one, deserving to receive updates once every other year or so.

Underlying the dataset, a broad range of documentation on water-level data exists on account of the large diversity of studies for which this data was collected. For some fields in the workbook the documentation is consistent for all samples, such as information on the geographic location of the sample, the sample age and information on the stratigraphical position of the sample (HOLSEA datasheet Section C. Fields related to horizontal position of RSL and Section D.1). For many other fields, it is much harder to be fully consistent, for example where uncertainties in depth and absolute elevation of the sample were considered. In some original studies, this information was thoroughly documented, while in others it was not included. Therefore, the uncertainties in sample depth have been re-calculated using the standard calculations provided by the HOLSEA workbook format. The fields related to the depth-related uncertainties (Section D.2 and D.3 in the HOLSEA workbook) and uncertainties in absolute elevation have partially been added.

The second part of the HOLSEA datasheet contains almost exclusively columns marked as interpretation columns (Section D.4 to D.7 in the HOLSEA workbook). This is the section where the additions of the dataset reported in this paper are documented. To align the documentation of this data, the metadata was iteratively reviewed. Specifically with regard to the

interpretation of the samples as either GWL, ULD or SLIP an effort was made to expand the dataset. The quality of the data depends strongly on the sampling method, sampling depth and what material was used for dating (e.g., bulk or macrofossils). The question arises if sampled material always represents the actual drowning surface. To prevent such ambiguity where possible, we recommend using a systematic approach for future sampling and dating of basal peat layers, in line with what is proposed by Quik et al. (2022; developed for relatively inland peats).

In few original publications, information on the tidal regime near the sampling site is included. It is understandable that this has not been standard practice, since not all samples were originally collected for water-level and sea-level reconstruction purposes. The HOLSEA-NL data base is set up to facilitate incorporating tidal information, and for all SLIP samples, this information is now provided. In addition to the current MHW level, an effort was made to provide the palaeo-tidal MHW level for these samples as well (as described in Sect. 4.1.2). Similarly, the database accommodates specification of basin subsidence and human-induced subsidence corrections - with respective values taken in from external data products for this (as described in Sect. 4.1.3-4). This provides transparent documentation on vertical corrections, their uncertainties, and the optionality of using them, enabling users to assess vertical corrections individually - which was one of the aims of this paper. Additionally, the transparent documentation of the different steps helps with the interpretation of the data and its uncertainties.

6.2 Data usage

Providing an overview of water-level data in the Netherlands with transparent documentation on the variety of adjustments needed and optional to transform raw data into sea-level indicators, was a main aim in the paper, fulfilled by publishing (De Wit and Cohen, 2024) and documenting (this paper) the HOLSEA-NL database. In this final section, some foreseen usages of the database will be briefly discussed.

First, the data set is intended to be used for relative sea-level reconstruction. For this the SLIPs, ULD and LLD are relevant input as well as the different tidal corrections (palaeo-tidal or using current MHW). In addition, it is possible to apply a basin subsidence correction, to eliminate the effect of the sinking of the North Sea basin out of the RSLR signal. Moreover, the increase in spatial and temporal coverage of the sea-level data, makes it possible to study patterns in the sea-level rise, such as tidal dampening (FBE) (Van de Plassche, 1995) and the river gradient effect (Louwe Kooijmans, 1972). Especially in the northern parts of the study area there is now more regional data, from which a start can be made to constrain the timing and extent of FBE sub regionally (as advocated for in Vis et al., 2015).

A second main application is to use the relative water-level rise documented through the data set, for reconstructing regional scale subsidence patterns. As mentioned and illustrated in Sect. 5.2, spatial intercomparison of rising trends in the data have revealed overprints of differential subsidence (Figure 9 and Figure 10). Over the Holocene these are attributed to GIA mainly, with tectonic subsidence a background component especially in W and NW sectors of the study area. Many earlier sea-level

data and GIA modelling combining studies stand example of the importance of comparing geological data with numerical GIA modelling output, to verify and constrain the modelling insights (e.g., Shennan and Horton, 2002; Vink et al., 2007; Bradley et al., 2011). Vice versa, modelling forecasts depths of sea-level indicators of given age in data scarce regions. With both data coverage and GIA modelling spatio-temporal resolutions increasing, geological data and modelling derived insights should be
780   expected to slowly converge. The increase in sea-level data density demonstrated by the HOLSEA-NL dataset (this paper), and specifically the better coverage and more uniform assessment of data from the northern half of the Netherlands, will provide more input to constrain GIA modelling output on a spatial scale. Conversely, a better understanding of the GIA signal in the Netherlands, will aid in untangling the Holocene relative sea-level rise signal into constituent components.

785   Apart from regional scale sea-level and subsidence reconstructions, the data set can also be used for reconstructing groundwater levels sub-regionally: in inland areas of the coastal plain, in the Rhine-Meuse delta sector, and throughout the coastal plain. In that case all indicator types provide input, and not the RSL but the GWL (i.e., without tidal correction) is used. Reconstructing local groundwater levels is the more direct approach when 3D mapping of the build-up of the Holocene wedge is the application and for studying spatial patterns in the relative water level rise (similar to Cohen, 2005; Koster et al., 2017). This is particularly
790   true for the Rhine-Meuse delta where previous work on water level indicator data has shown water-level isochrones to display a downstream gradient (Louwe Kooijmans, 1972; Van Dijk et al., 1991). As a first step, we have explicitly labeled the data points to which this applies. In Sect. 5 this was presented with focus on deselection of such data points when exploring the dataset for spatial patterns and differences in MHW and MSL. Applications that explicitly include this data and that investigate and analyze variability in groundwater table elevations in space and time in the delta flood basins may also be envisaged (e.g.,
795   Van Asselen et al., 2017). In future investigations it might be possible to further analyze the river gradient effect and potentially correct inland water-level indicators for this process, for instance to extend differential subsidence analysis inland. Even without explicit correction, groundwater level isochrones of Rhine-Meuse delta flood basins peats have been used for analysing local vertical displacement of deposits. For example, to quantify fault offsets across the Peel Boundary Fault zone (Cohen, 2005) and to quantify degree of compaction-lowering of intercalated peats at shorter and further distance of burying deltaic
800   river branches (Van Asselen, 2011). Furthermore, these water level isochrones based on basal peat data have provided context for many archaeological excavating studies on the Mesolithic and Neolithic of the Rhine-Meuse delta (e.g., Louwe Kooijmans, 1972; Van der Woude, 1983; Verbruggen, 1992) as well as in the further coastal plain (e.g., Peeters, 2007; Van den Biggelaar et al., 2015).

7. Conclusion

805   This paper presents a compilation of Holocene coastal water-level indicator data from the Netherlands, brought together in a consistent format, using the HOLSEA workbook format. The workbook was expanded and complemented, and processing protocols adapted, to accommodate information on more inland water-level data as well to make the compilation suitable for

reconstructing relative groundwater rise, sea-level rise and regional subsidence. The compilation processed legacy data, as well as more recently produced data, in majority (>600 out of 712 points) not earlier processed with HOLSEA protocols (104

810   datapoints from Zuid Holland being the exception).

Careful and systematic incorporation of sample properties from extensive scattered documentation on individual samples from more than 110 source papers and reports, and a considerable amount of specialised literature on GWL and MSL indicative meaning of peat data from the Dutch setting, allowed for consistent treatment and specification of different depth adjustment

815   possibilities for each sample. The classification of the data in SLIPs, ULDs and LLDs, especially when combined with the locational information and subregion-labelling should help guide data users in making the right sub selections for their application.

In conclusion, this paper and the versatile structure of the new HOLSEA-NL data set make the water-level data suitable for

820   multiple usages. On top of that, its open accessibility and documentation makes future expansion of the data set possible. In northeastern, northwestern, and southwestern parts of the Netherlands there are still considerable gaps that would welcome improved coverage with Holocene water level markers, also for cross validating the current data. Overall, the open access data set can provide input and context for future Holocene water-level and sea-level research, bridging between the large amount of legacy data and newly collected indicator data and unifying these data in a consistent format.

825   **Data availability**

The HOLSEA-NL database (https://zenodo.org/doi/10.5281/zenodo.11098446; De Wit and Cohen (2024)), as a scientific product, is open-access available (CC-BY). The data set was compiled by the authors, and contains abundant referencing to a great variety of source publications (part scientific, and referred to in this paper too, part applied regional reports and/or from institutional databases, referencing not doubled in this paper). The HOLSEA-NL database format is compliant with field
830   descriptions in https://www.holsea.org/archive-your-data: see Sect. 4 for added fields specific to our compiling and the Dutch geological setting.

Team list. Kim de Wit, Kim M. Cohen, Roderik S. W. van de Wal

Author contribution. KW and KMC reviewed literature related to data inventory and curated the data set. KW prepared figures, tables and original draft. All authors edited the manuscript and contributed to conceptualization of the manuscript and
835   designing key figures.

Competing interests. The authors declare that they have no conflict of interest.

Acknowledgements. The research presented in this paper is part of the project Living on Soft Soils: Subsidence and Society (grantnr.: NWA.1160.18.259). This project is funded by the Dutch Research Council (NWO-NWA-ORC), Utrecht University, Wageningen University, Delft University of Technology, Ministry of Infrastructure & Water Management, Ministry of the
840   Interior & Kingdom Relations, Deltares, Wageningen Environmental Research, TNO-Geological Survey of The Netherlands,

STOWA, Water Authority: Hoogheemraadschap de Stichtse Rijnlanden, Water Authority: Drents Overijsselse Delta, Province of Utrecht, Province of Zuid-Holland, Municipality of Gouda, Platform Soft Soil, Sweco, Tauw BV, NAM.

References

845 Autin, W. J.: Stratigraphic analysis and paleoenvironmental implications of the Wijchen Member in the lower Rhine-Meuse Valley of the Netherlands, Netherlands Journal of Geosciences, 87, 291–307, https://doi.org/10.1017/S0016774600023362, 2008.

Beets, D. J. and Van der Spek, A. J. F.: The Holocene evolution of the barrier and the back-barrier basins of Belgium and the Netherlands as a function of late Weichselian morphology, relative sea-level rise and sediment supply, Netherlands Journal of 850 Geosciences, 79, 3–16, https://doi.org/10.1017/S0016774600021533, 2000.

Behre, K.-E.: A new Holocene sea-level curve for the southern North Sea, SBOR, 36, 82–102, https://doi.org/10.1080/03009480600923386, 2007.

Bennema, J.: Bodem-en zeespiegelbewegingen in het Nederlandse kustgebied, Wageningen University and Research, 1954.

Bennema, J. and Pons, L.: Donken, fluviatiel Laagterras en Eemzee-afzettingen in het westelijk gebied van de grote rivieren, 855 Boor en Spade, 5, 126–137, 1952.

Berendsen, H. J. A. and Stouthamer, E.: Palaeogeographic development of the Rhine-Meuse delta, The Netherlands / Henk J.A. Berendsen & Esther Stouthamer., Koninklijke Van Gorcum, Assen, xi+268 pp., 2001.

Berendsen, H. J. A. and Stouthamer, E.: Paleogeographic evolution and avulsion history of the Holocene Rhine-Meuse delta, The Netherlands, Netherlands Journal of Geosciences, 81, 97–112, https://doi.org/10.1017/S0016774600020606, 2002.

860 Berendsen, H. J. A., Makaske, B., Van de Plassche, O., Van Ree, M. H. M., Das, S., Van Dongen, M., Ploumen, S., and Schoenmakers, W.: New groundwater-level rise data from the Rhine-Meuse delta – implications for the reconstruction of Holocene relative mean sea-level rise and differential land-level movements, Netherlands Journal of Geosciences, 86, 333–354, https://doi.org/10.1017/S0016774600023568, 2007.

Bos, I. J., Busschers, F. S., and Hoek, W. Z.: Organic-facies determination: a key for understanding facies distribution in the 865 basal peat layer of the Holocene Rhine-Meuse delta, The Netherlands, Sedimentology, 59, 676–703, https://doi.org/10.1111/j.1365-3091.2011.01271.x, 2012.

Bradley, S. L., Milne, G. A., Shennan, I., and Edwards, R.: An improved glacial isostatic adjustment model for the British Isles: GLACIAL ISOSTATIC ADJUSTMENT MODEL FOR THE BRITISH ISLES, J. Quaternary Sci., 26, 541–552, https://doi.org/10.1002/jqs.1481, 2011.

870 Bronk Ramsey, C.: Deposition models for chronological records, Quaternary Science Reviews, 27, 42–60, https://doi.org/10.1016/j.quascirev.2007.01.019, 2008.

Bronk Ramsey, C.: Bayesian analysis of radiocarbon dates, Radiocarbon, 51, 337–360, https://doi.org/10.1017/S0033822200033865, 2009.

Bungenstock, F., Freund, H., and Bartholomä, A.: Holocene relative sea-level data for the East Frisian barrier coast, NW 875 Germany, southern North Sea, Netherlands Journal of Geosciences, 100, e16, https://doi.org/10.1017/njg.2021.11, 2021.

Busschers, F. S., Kasse, C., van Balen, R. T., Vandenberghe, J., Cohen, K. M., Weerts, H. J. T., Wallinga, J., Johns, C., Cleveringa, P., and Bunnik, F. P. M.: Late Pleistocene evolution of the Rhine-Meuse system in the southern North Sea basin: imprints of climate change, sea-level oscillation and glacio-isostacy, Quaternary Science Reviews, 26, 3216–3248, https://doi.org/10.1016/j.quascirev.2007.07.013, 2007.

880   Cahill, N., Kemp, A. C., Horton, B. P., and Parnell, A. C.: Modeling sea-level change using errors-in-variables integrated Gaussian processes, The Annals of Applied Statistics, 9, 547–571, https://doi.org/10.1214/15-AOAS824, 2015.

Cohen, K. M.: 3D Geostatistical Interpolation and Geological Interpretation of Paleo-Groundwater Rise in the Holocene Coastal Prism in the Netherlands, in: River Deltas–Concepts, Models, and Examples, vol. 83, edited by: Giosan, L. and Bhattacharya, J. P., SEPM Society for Sedimentary Geology, 0, https://doi.org/10.2110/pec.05.83.0341, 2005.

885   Cohen, K. M., Schokker, J., Hijma, M. P., Koster, K., Pierik, H. J., Vos, P. C., Erkens, G., and Stafleu, J.: Landschapskaarten en hoogtemodellen naar periode en diepte voor archeologisch gebruik in Holoceen-afgedekte delen van Nederland, https://doi.org/10.17026/dans-zck-y7ww, 2017a.

Cohen, K. M., Dambrink, R., De Bruijn, R., Marges, V. C., Erkens, G., Pierik, H. J., Koster, K., Stafleu, J., Schokker, J., Hijma, M. P., Lauwerier, R. C. G. M., Eerden, M. C., Groenewoudt, B. J., Lascaris, M. A., Rensink, E., Smit, B. I., Speleers, 890   B. P., and Van Doesburg, J.: Mapping buried Holocene landscapes: past lowland environments, palaeoDEMs and preservation in GIS, 55, 73–95, 2017b.

Cohen, K. M., Cartelle, V., Barnett, R., Busschers, F. S., and Barlow, N. L. M.: Last Interglacial sea-level data points from Northwest Europe, Palaeooceanography, palaeoclimatology, https://doi.org/10.5194/essd-2021-390, 2021.

Creel, R. C., Austermann, J., Khan, N. S., D'Andrea, W. J., Balascio, N., Dyer, B., Ashe, E., and Menke, W.: Postglacial 895   relative sea level change in Norway, Quaternary Science Reviews, 282, 107422, https://doi.org/10.1016/j.quascirev.2022.107422, 2022.

De Moor, J., Bos, J. A. A., Bouman, M., Moolhuizen, C., Exaltus, R. P., Maartense, F. P. A., and Van der Linden, T. J. M.: Definitief Archeologisch Onderzoek in het tracé van de Hanzelijn in het Nieuwe Land, Een interdisciplinaire geo-archeologische waardering van het begraven landschap van Oostelijk Flevoland, 2009.

900   De Wit, K. and Cohen, K. M.: HOLSEA-NL: Holocene water level and sea-level indicator dataset for the Netherlands (v1.0), https://doi.org/10.5281/zenodo.11098447, 2024.

Ente, P. J., Zagwijn, W. H., and Mook, W. G.: The Calais deposits in the vicinity of wieringen and the geogenisis of Northern North Holland, Geologie en Mijnbouw, 54, 1–14, 1975.

Erkens, G., Van der Meulen, M. J., and Middelkoop, H.: Double trouble: subsidence and CO2 respiration due to 1,000 years 905   of Dutch coastal peatlands cultivation, Hydrogeol J, 24, 551–568, https://doi.org/10.1007/s10040-016-1380-4, 2016.

Gotjé, W.: De Holocene laagveenontwikkeling in de randzone van de Nederlandse kustvlakte (Noordoostpolder), 1993.

Hamburg, T. and Knippenberg, S.: Proefsleuven op drie locaties binnen het tracé van de Hanzelijn 'Oude Land,' 2006.

Heaton, T. J., Köhler, P., Butzin, M., Bard, E., Reimer, R. W., Austin, W. E. N., Ramsey, C. B., Grootes, P. M., Hughen, K. A., Kromer, B., Reimer, P. J., Adkins, J., Burke, A., Cook, M. S., Olsen, J., and Skinner, L. C.: Marine20—The Marine 910   Radiocarbon Age Calibration Curve (0–55,000 cal BP), Radiocarbon, 62, 779–820, https://doi.org/10.1017/RDC.2020.68, 2020.

Hijma, M. P. and Cohen, K. M.: Timing and magnitude of the sea-level jump preluding the 8200 yr event, Geology, 38, 275–278, https://doi.org/10.1130/G30439.1, 2010.

Hijma, M. P. and Cohen, K. M.: Holocene sea-level database for the Rhine-Meuse Delta, The Netherlands: Implications for the pre-8.2 ka sea-level jump, Quaternary Science Reviews, 214, 68–86, https://doi.org/10.1016/j.quascirev.2019.05.001, 2019.

Hijma, M. P., Engelhart, S. E., Törnqvist, T. E., Horton, B. P., Hu, P., and Hill, D. F.: A protocol for a geological sea-level database, in: Handbook of Sea-Level Research, John Wiley & Sons, Ltd, 536–553, https://doi.org/10.1002/9781118452547.ch34, 2015.

Hoek, W. Z.: Late-glacial and early Holocene climatic events and chronology of vegetation development in the Netherlands, Veget Hist Archaebot, 6, 197–213, https://doi.org/10.1007/BF01370442, 1997.

Jelgersma, S.: Holocene sea-level changes in the Netherlands, Ph. D. dissertation, Leiden University, Leiden, 1961.

Kasse, C. and Aalbersberg, G.: A complete Late Weichselian and Holocene record of aeolian coversands, drift sands and soils forced by climate change and human impact, Ossendrecht, the Netherlands, Netherlands Journal of Geosciences, 98, e4, https://doi.org/10.1017/njg.2019.3, 2019.

Khan, N. S., Horton, B. P., Engelhart, S., Rovere, A., Vacchi, M., Ashe, E. L., Törnqvist, T. E., Dutton, A., Hijma, M. P., and Shennan, I.: Inception of a global atlas of sea levels since the Last Glacial Maximum, Quaternary Science Reviews, 220, 359–371, https://doi.org/10.1016/j.quascirev.2019.07.016, 2019.

Kiden, P.: Holocene relative sea-level change and crustal movement in the southwestern Netherlands, Marine Geology, 124, 21–41, https://doi.org/10.1016/0025-3227(95)00030-3, 1995.

Kiden, P., Denys, L., and Johnston, P.: Late Quaternary sea-level change and isostatic and tectonic land movements along the Belgian-Dutch North Sea coast: geological data and model results, J. Quaternary Sci., 17, 535–546, https://doi.org/10.1002/jqs.709, 2002.

Kiden, P., Makaske, B., and Van de Plassche, O.: Waarom verschillen de zeespiegelreconstructies voor Nederland?, Grondboor & Hamer, 62, 54–61, 2008.

Kooi, H., Johnston, P., Lambeck, K., Smither, C., and Ronald Molendijk: Geological causes of recent (~100 yr) vertical land movement in the Netherlands, Tectonophysics, 299, 297–316, https://doi.org/10.1016/S0040-1951(98)00209-1, 1998.

Koster, K., Stafleu, J., and Cohen, K. M.: Generic 3D interpolation of Holocene base-level rise and provision of accommodation space, developed for the Netherlands coastal plain and infilled palaeovalleys, Basin Res, 29, 775–797, https://doi.org/10.1111/bre.12202, 2017.

Lambeck, K.: Late Devensian and Holocene shorelines of the British Isles and North Sea from models of glacio-hydro-isostatic rebound, JGS, 152, 437–448, https://doi.org/10.1144/gsjgs.152.3.0437, 1995.

Louwe Kooijmans, L.: The Rhine/Meuse Delta. Four studies on its prehistoric occupation and Holocene geology, Leiden University, Leiden, 1972.

Makaske, B. and Maas, G. J.: Different hydrological controls causing variable rates of Holocene peat growth in a lowland valley system, north-eastern Netherlands; implications for valley peatland restoration, The Holocene, 33, 960–974, https://doi.org/10.1177/09596836231169985, 2023.

Makaske, B., Smeerdijk, D. G. V., Peeters, H., Mulder, J. R., and Spek, T.: Relative water-level rise in the Flevo lagoon (The Netherlands), 5300-2000 cal. yr BC: an evaluation of new and existing basal peat time-depth data, Netherlands Journal of Geosciences, 82, 115–131, https://doi.org/10.1017/S0016774600020680, 2003.

Meijles, E. W., Kiden, P., Streurman, H.-J., Van der Plicht, J., Vos, P. C., Gehrels, W. R., and Kopp, R. E.: Holocene relative mean sea-level changes in the Wadden Sea area, northern Netherlands, Journal of Quaternary Science, 33, 905–923, https://doi.org/10.1002/jqs.3068, 2018.

NAM: Aanvraag Instemming Winningsplan Gaag-Monster, 2017.

NAM: Statusrapport 2020 en Prognose tot het jaar 2080, 2020.

Peeters, J., Busschers, F. S., Stouthamer, E., Bosch, J. H. A., Van den Berg, M. W., Wallinga, J., Versendaal, A. J., Bunnik, F. P. M., and Middelkoop, H.: Sedimentary architecture and chronostratigraphy of a late Quaternary incised-valley fill: A case study of the late Middle and Late Pleistocene Rhine system in the Netherlands, Quaternary Science Reviews, 131, 211–236, https://doi.org/10.1016/j.quascirev.2015.10.015, 2016.

Peeters, J. H. M.: Hoge Vaart-A27 in context: towards a model of mesolithic - neolithic land use dynamics as a framework for archaeological heritage management, AmsersfoortRijksdienst voor Archeologie, Cultuurlandschap en Monumenten, 2007.

Pierik, H. J. and Cohen, K. M.: The use of geological, geomorphological and soil mapping products in palaeolandscape reconstructions for the Netherlands, Netherlands Journal of Geosciences, 99, e9, https://doi.org/10.1017/njg.2020.8, 2020.

Pierik, H. J., Cohen, K. M., Vos, P. C., Van der Spek, A. J. F., and Stouthamer, E.: Late Holocene coastal-plain evolution of the Netherlands: the role of natural preconditions in human-induced sea ingressions, Proceedings of the Geologists' Association, 128, 180–197, https://doi.org/10.1016/j.pgeola.2016.12.002, 2017.

Pons, L. J. and Wiggers, A. J.: The holocene wordingsgeschiedenis van Noord-Holland en het Zuiderzeegebied = The holocene genesis of the province of North-Holland and the Zuyder Sea region, 1960.

Quik, C., Van der Velde, Y., Harkema, T., Van der Plicht, H., Quik, J., Van Beek, R., and Wallinga, J.: Using legacy data to reconstruct the past? Rescue, rigour and reuse in peatland geochronology, Earth Surf Processes Landf, 46, 2607–2631, https://doi.org/10.1002/esp.5196, 2021.

Quik, C., Palstra, S. W. L., Van Beek, R., Van der Velde, Y., Candel, J. H. J., Van der Linden, M., Kubiak-Martens, L., Swindles, G. T., Makaske, B., and Wallinga, J.: Dating basal peat: The geochronology of peat initiation revisited, Quaternary Geochronology, 72, 101278, https://doi.org/10.1016/j.quageo.2022.101278, 2022.

Shennan, I.: Interpretation of Flandrian sea-level data from the Fenland, England, Proceedings of the Geologists' Association, 93, 53–63, https://doi.org/10.1016/S0016-7878(82)80032-1, 1982.

Shennan, I. and Horton, B.: Holocene land- and sea-level changes in Great Britain, J Quaternary Science, 17, 511–526, https://doi.org/10.1002/jqs.710, 2002.

Shennan, I., Lambeck, K., Flather, R., Horton, B., McArthur, J., Innes, J., Lloyd, J., Rutherford, M., and Wingfield, R.: Modelling western North Sea palaeogeographies and tidal changes during the Holocene, SP, 166, 299–319, https://doi.org/10.1144/GSL.SP.2000.166.01.15, 2000.

Simon, K. M. and Riva, R. E. M.: Uncertainty Estimation in Regional Models of Long-Term GIA Uplift and Sea Level Change: An Overview, Journal of Geophysical Research: Solid Earth, 125, e2019JB018983, https://doi.org/10.1029/2019JB018983, 2020.

985 Steffelbauer, D. B., Riva, R. E. M., Timmermans, J. S., Kwakkel, J. H., and Bakker, M.: Evidence of regional sea-level rise acceleration for the North Sea, Environ. Res. Lett., 17, 074002, https://doi.org/10.1088/1748-9326/ac753a, 2022.

Stouthamer, E. and Berendsen, H. J. A.: Factors Controlling the Holocene Avulsion History of the Rhine-Meuse Delta (The Netherlands), Journal of Sedimentary Research, 70, 1051–1064, https://doi.org/10.1306/033000701051, 2000.

Törnqvist, T., Weerts, H. J. T., and Berendsen, H.: Definition of two new members in the upper Kreftenheye and Twente
990 Formations (Quaternary, the Netherlands): a final solution to persistent confusion?, Geologie en Mijnbouw, 72, 251–264, 1994.

Törnqvist, T. E., Van Ree, M. H. M., Van 'T Veer, R., and Van Geel, B.: Improving Methodology for High-Resolution Reconstruction of Sea-Level Rise and Neotectonics by Paleoecological Analysis and AMS ^{14}C Dating of Basal Peats, Quat. res., 49, 72–85, https://doi.org/10.1006/qres.1997.1938, 1998.

995 Törnqvist, T. E., González, J. L., Newsom, L. A., Van der Borg, K., De Jong, A. F. M., and Kurnik, C. W.: Deciphering Holocene sea-level history on the U.S. Gulf Coast: A high-resolution record from the Mississippi Delta, GSA Bulletin, 116, 1026–1039, https://doi.org/10.1130/B2525478.1, 2004.

Uehara, K., Scourse, J. D., Horsburgh, K. J., Lambeck, K., and Purcell, A. P.: Tidal evolution of the northwest European shelf seas from the Last Glacial Maximum to the present, Journal of Geophysical Research: Oceans, 111,
1000 https://doi.org/10.1029/2006JC003531, 2006.

Van Asselen, S.: The contribution of peat compaction to total basin subsidence: implications for the provision of accommodation space in organic-rich deltas: The contribution of peat compaction to basin subsidence, Basin Research, 23, 239–255, https://doi.org/10.1111/j.1365-2117.2010.00482.x, 2011.

Van Asselen, S., Stouthamer, E., and Van Asch, Th. W. J.: Effects of peat compaction on delta evolution: A review on
1005 processes, responses, measuring and modeling, Earth-Science Reviews, 92, 35–51, https://doi.org/10.1016/j.earscirev.2008.11.001, 2009.

Van Asselen, S., Cohen, K. M., and Stouthamer, E.: The impact of avulsion on groundwater level and peat formation in delta floodbasins during the middle-Holocene transgression in the Rhine-Meuse delta, The Netherlands, The Holocene, 27, 1694–1706, https://doi.org/10.1177/0959683617702224, 2017.

1010 Van de Plassche, O.: Compaction and Other Sources of Error in Obtaining Sea-Level Data: Some Results and Consequences, E&G Quaternary Science Journal, 30, 171–182, https://doi.org/10.3285/eg.30.1.14, 1980.

Van de Plassche, O.: Sea-level change and water-level movements in the Netherlands during the Holocene, Mededelingen Rijks Geologische Dienst, 36, 1–93, 1982.

Van de Plassche, O.: Sea-level research : a manual for the collection and evaluation of data, Geo Books, Norwich, 1986.

1015 Van de Plassche, O.: Evolution of the intra-coastal tidal range in the Rhine-Meuse delta and Flevo Lagoon, 5700-3000 yrs cal B.C., Marine Geology, 124, 113–128, https://doi.org/10.1016/0025-3227(95)00035-W, 1995.

Van de Plassche, O., Bohncke, S. J. P., Makaske, B., and Van der Plicht, J.: Water-level changes in the Flevo area, central Netherlands (5300–1500 BC): implications for relative mean sea-level rise in the Western Netherlands, Quaternary International, 133–134, 77–93, https://doi.org/10.1016/j.quaint.2004.10.009, 2005.

1020 Van de Plassche, O., Makaske, B., Hoek, W. Z., Konert, M., and Van Der Plicht, J.: Mid-Holocene water-level changes in the lower Rhine-Meuse delta (western Netherlands): implications for the reconstruction of relative mean sea-level rise, palaeoriver-gradients and coastal evolution, Netherlands Journal of Geosciences, 89, 3–20, https://doi.org/10.1017/S0016774600000780, 2010.

Van den Berg, M. and Beets, D.: Saalian glacial deposits and morphology in The Netherlands, Tills and Glaciotectonics. 1025 Balkema, Rotterdam, 235–251, 1987.

Van den Biggelaar, D. F. A. M., Kluiving, S. J., Bohncke, S. J. P., Van Balen, R. T., Kasse, C., Prins, M. A., and Kolen, J.: Landscape potential for the adoption of crop cultivation: Role of local soil properties and groundwater table rise during 6000–5400 BP in Flevoland (central Netherlands), Quaternary International, 367, 77–95, https://doi.org/10.1016/j.quaint.2014.09.063, 2015.

1030 Van den Brenk, S., Huisman, H., Willemse, N. W., Smit, B., and Van Os, B. J. H.: Magnetometer mapping of drowned prehistoric landscapes for Archaeological Heritage Management in the Netherlands, Archaeological Prospection, n/a, https://doi.org/10.1002/arp.1925, 2023.

Van der Meulen, M. J., Doornenbal, J. C., Gunnink, J. L., Stafleu, J., Schokker, J., Vernes, R. W., Geer, F. C. van, Gessel, S. F. van, Heteren, S. van, Leeuwen, R. J. W. van, Bakker, M. a. J., Bogaard, P. J. F., Busschers, F. S., Griffioen, J., Gruijters, S. 1035 H. L. L., Kiden, P., Schroot, B. M., Simmelink, H. J., Berkel, W. O. van, Krogt, R. A. A. van der, Westerhoff, W. E., and Daalen, T. M. van: 3D geology in a 2D country: perspectives for geological surveying in the Netherlands, Netherlands Journal of Geosciences, 92, 217–241, https://doi.org/10.1017/S0016774600000184, 2013.

Van der Molen, J. and De Swart, H. E.: Holocene tidal conditions and tide-induced sand transport in the southern North Sea, Journal of Geophysical Research: Oceans, 106, 9339–9362, https://doi.org/10.1029/2000JC000488, 2001.

1040 Van der Woude, J. D. (Jan D.: Holocene paleoenvironmental evolution of a perimarine fluviatile area: geology and paleobotany of the area surrounding the archeological excavation at the Hazendonk river dune (western Netherlands), Leiden U.P. Modderman Stichting., Leiden, 124 pp., 1983.

Van Dijk, G. J., Berendsen, H. J. A., and Roeleveld, W.: Holocene water level development in The Netherlands' river area; implications for sea-level reconstruction, Geologie en Mijnbouw, 70, 311–326, 1991.

1045 Van Lil, R.: Aanleg N23 tussen Lelystad en Dronten, 2008.

Van Straaten, L.: Radiocarbon datings and changes of sea level at Velzen (Netherlands), Geologie en Mijnbouw (NW. SER.), 16, 247–253, 1954.

Van Veen, J.: Eb-en vloedschaar systemen in de Nederlandse getijwateren, Tijdschrift Koninklijk Nederlands Aardrijkskundig Genootschap, 67, 303–325, 1950.

1050 Van Veen, J., Van der Spek, A. J. F., Stive, M. J. F., and Zitman, T.: Ebb and Flood Channel Systems in the Netherlands Tidal Waters, coas, 2005, 1107–1120, https://doi.org/10.2112/04-0394.1, 2005.

Verbruggen, M.: Geoarchaeological prospection of the Rommertsdonk, Analecta Praehistorica Leidensia 25: The end of our third decade: Papers written on the occasion of the 30th anniversary of the Institutte of prehistory, volume I, 25, 119–128, 1992.

1055   Vermeersen, B. L. A., Slangen, A. B. A., Gerkema, T., Baart, F., Cohen, K. M., Dangendorf, S., Duran-Matute, M., Frederikse, T., Grinsted, A., Hijma, M. P., Jevrejeva, S., Kiden, P., Kleinherenbrink, M., Meijles, E. W., Palmer, M. D., Rietbroek, R., Riva, R. E. M., Schulz, E., Slobbe, D. C., Simpson, M. J. R., Sterlini, P., Stocchi, P., Van de Wal, R. S. W., and Van der Wegen, M.: Sea-level change in the Dutch Wadden Sea, Netherlands Journal of Geosciences, 97, 79–127, https://doi.org/10.1017/njg.2018.7, 2018.

1060   Vink, A., Steffen, H., Reinhardt, L., and Kaufmann, G.: Holocene relative sea-level change, isostatic subsidence and the radial viscosity structure of the mantle of northwest Europe (Belgium, the Netherlands, Germany, southern North Sea), Quaternary Science Reviews, 26, 3249–3275, https://doi.org/10.1016/j.quascirev.2007.07.014, 2007.

Vis, G.-J., Cohen, K. M., Westerhoff, W. E., Veen, J. H. T., Hijma, M. P., van der Spek, A. J. F., and Vos, P. C.: Paleogeography, in: Handbook of Sea-Level Research, John Wiley & Sons, Ltd, 514–535, 1065   https://doi.org/10.1002/9781118452547.ch33, 2015.

Vogel, J. C. and Waterbolk, H. T.: Groningen Radiocarbon Dates IV, Radiocarbon, 5, 163–202, https://doi.org/10.1017/S0033822200036857, 1963.

Vos, P.: Origin of the Dutch coastal landscape: Long-term landscape evolution of the Netherlands during the Holocene, described and visualized in national, regional and local palaeogeographical map series, Barkhuis, 373 pp., 2015.

1070   Vos, P., Van der Meulen, M., Weerts, H., and Bazelmans, J.: Atlas of the Holocene Netherlands, landscape and habitation since the last ice age, Amsterdam University Press, Amsterdam, 96 pp., 2020.

Vos, P. C. and Gerrets, D. A.: Archaeology: a major tool in the reconstruction of the coastal evolution of Westergo (northern Netherlands), Quaternary International, 133, 61–75, 2005.

Vos, P. C. and Nieuwhof, A.: Late-Holocene sea-level reconstruction (1200 BC–AD 100) in the Westergo terp region of the 1075   northern Netherlands, Netherlands Journal of Geosciences, 100, e3, https://doi.org/10.1017/njg.2021.1, 2021.

Ward, S. L., Neill, S. P., Scourse, J. D., Bradley, S. L., and Uehara, K.: Sensitivity of palaeotidal models of the northwest European shelf seas to glacial isostatic adjustment since the Last Glacial Maximum, Quaternary Science Reviews, 151, 198–211, https://doi.org/10.1016/j.quascirev.2016.08.034, 2016.

Wiggers, A. J.: De wording van het Noordoostpoldergebied: een onderzoek naar de physisch-geografische ontwikkeling van 1080   een sedimentair gebied, Tjeenk Willink, 1955.

Wolfert, H. P. and Maas, G. J.: Downstream changes of meandering styles in the lower reaches of the River Vecht, the Netherlands, Netherlands Journal of Geosciences, 86, https://doi.org/10.1017/S0016774600077842, 2007.

Zagwijn, W. H.: The pleistocene of The Netherlands with special reference to glaciation and terrace formation, Quaternary Science Reviews, 5, 341–345, https://doi.org/10.1016/0277-3791(86)90195-2, 1986.

1085   Zonneveld, I. S.: De Brabantse Biesbosch: een studie van bodem en vegetatie van een zoetwatergetijdendelta, Wageningen University and Research, 1960.